Cumulative effects of channel correction and regulation on floodplain terrestrialisation patterns and connectivity

A. Tena, H. Piégay, G. Seignemartin, A. Barra, J.F. Berger, Brice Mourier, T. Winiarski

Cumulative effects of channel correction and regulation on floodplain terrestrialisation patterns and connectivity

Tena A.[1,*], Piégay H.[1], Seignemartin G.[2], Barra A.[3], Berger J.F.[3], Mourier B.[4], Winiarski T.[4]

[1] CNRS, UMR5600, Laboratoire EVS, Lyon, France

[2] Université Lyon 2, Laboratoire EVS, UMR5600, Lyon, France

[3] CNRS, UMR 5600, IRG-Université Lyon 2, Lyon, France.

[4] CNRS, UMR 5023, ENTPE - LEHNA, Vaux-en-Velin, France

Abstract: One of the main drivers of overbank fine deposition and floodplain formation is the hydrological connectivity between the channel and the floodplain. Channel correction (i.e., groyne field construction within the main flow channel and secondary channel disconnections) and flow regulation can typically lead to a disconnection of riverine floodplains and disturbances that directly affect terrestrialisation. Channel correction and flow regulation can sometimes occur successively, and it is challenging to distinguish the roles of each. This work attempts to assess the respective effects of two phases of channel regulation (correction versus flow regulation) on floodplain terrestrialisation by comparing three bypassed reaches of the Rhône, France (Pierre-Bénite, Péage-de-Roussillon and Donzère-Mondragon). We applied a transversal methodology coupled with GIS analysis (old maps, Orthophotos, DEM's, etc.) to understand processes of channel-planform evolution, conducted a sediment survey (metal rod) to assess floodplain terrestrialisation, and performed sediment sampling (manual auger) to obtain surface sediment metal content levels (X-ray Fluorescence and Inductively Coupled Plasma Mass Spectrometry). We found a general trend of channel narrowing within the three reaches, among which approximately 40% was found to be associated with correction works while 20% was attributed to flow lowering caused by channel bypassing. The number of flowing channels in all sections declined significantly, and local anabranching reaches evolved into very stable single thread channels. Overbank sedimentation declined significantly over the period, with very high sedimentation levels observed immediately after correction works and with very low sedimentation levels observed after diversion. We also found overbank flooding (in the number of days per year) decreased while fine sediment thickness increased. Similarly,

the highest concentrations of metals (Zc, Pb, and Cu) were found to be associated with a low connection frequency and vice versa. When similar 2-staged terrestrialisation patterns are observed in all three reaches, they differ in chronology and driving factors because of their longitudinal positioning and specific local conditions.

Keywords: Rhône River, river engineering, groyne fields, river regulation, connection frequency, sedimentation, metal content, river narrowing

1. Introduction

Rivers and their valleys have been historically modified and transformed in Europe and throughout the northern hemisphere to satisfy human demands for flood control, navigation, agriculture, and more recently hydro-electric power production and industry proposals. These activities have produced a series of transformations that have radically altered river morphologies and associated ecosystems (Petts, 1984, 1989; Dynesius and Nilsson, 1994; Nilsson and Berggren, 2000; Tockner and Stanfor,d 2002, Gregory, 2006). The main cause of the ecological alteration of rivers is hydrologic disconnection (Wohl, 2004) in its longitudinal, lateral and vertical dimensions (Ward, 1998). For example, navigation infrastructures such as artificial levees, canals, gravel dredges and flow regulation systems (Ward, 1998; Amoros and Bornette, 2002) typically lead to a lateral disconnection of riverine floodplains (Ward and Stanford, 1995; Cowx and Welcomme, 1998). This reduced lateral connectivity also decreases floodplain productivity, nutrient exchange, and dispersal of biota between the river and floodplain wetlands (Jenkins and Boulton, 2003). Moreover, floodplains also contribute as retention areas for flood water (Somlyódi, 2011) and groundwater storage (Stanford, 1998). Floodplains, by its nature, connect lotic, riparian and groundwater environments, and organisms relying in its habitats (i.e., fish, macroinvertebrates, etc.) and the disconnection of floodplain habitats can result in a decline in ecological diversity (Nijland and Cals, 2001;

55 Tockner and Stanford, 2002; Nilsson et al., 2005, Roni et al., 2019). Structures such as weirs
56 and dams that are created for hydropower production, drinking water supply, irrigation and
57 flood protection can interrupt the longitudinal continuity of rivers as a physical barrier to the
58 migration of fish and other biota, but also by altering the natural transfer of water and
59 sediment (Nilsson et al., 2005; Auble, Friedman and Scott, 1994; Nilsson and Jansson, 1995;
60 Nilsson, Jansson and Zinko 1997; Jansson, Nilsson and Renöfält, 2000; Merritt and Cooper
61 2000). In general terms, ecological consequences of hydromorphological alterations include
62 the reduction of complexity, dynamism and biodiversity (Elosegi et al., 2010).

63 Many different techniques have been used to improve or rehabilitate floodplains and their
64 associated habitats. These include but are not limited to facilitating river continuity (i.e.,
65 longitudinal connectivity), floodplain reconnection (i.e., lateral connectivity) and the re-
66 naturalization of flow regimes below dams (i.e., inter and intra annual variability, flood
67 magnitude and frequency) (Tockner, Schiemer and Ward, 1998; Simons et al., 2001; Coops et
68 al., 2006; Kondolf et al., 2006; Shields et al., 2011; Magilligan et al., 2016). In addition, other
69 techniques such as riparian planting or invasive species removal, and the placement of logs,
70 logjams, boulders and other structures are commonly implemented as part of floodplain
71 restoration (Roni et al., 2019). The importance of lateral connectivity between a floodplain and
72 its main channel has been highlighted as the hydrological connectivity of river–floodplain
73 ecosystems, and is linked to high levels of biological diversity (Ward, 1998; Schiemer et al.,
74 1999; Ward et al., 1999). Lateral in-channel hydraulic structures (dikes, riprap protection, and
75 groyne fields) limit potential shifting (Depret et al., 2017) and floodplain rejuvenation,
76 promoting continuous overbank fine aggradation and disconnection from potential effects on
77 river discharge capacities. The removal of such infrastructures can thus help re-connect
78 floodplains and side channels with the main river stem and restore lateral connectivity.

79 Artificial reconnection can however, also have negative effects (Wohl et al., 2005; Kondolf et
80 al., 2006). For example, artificial floodplain reconnection achieved through the removal of in-

channel hydraulic structures involves addressing other critical questions linked to sediment quantity and quality management. These structures may act as sediment traps where fine deposited sediment is often contaminated with pollutants or nutrients (Schwartz and Kozerski, 2003). Hence, measures based on groyne, riprap and dike removal for re-naturalising fluvial processes may remobilize and distribute contaminated sediments, affecting downstream river reaches. This is one of the main drawbacks of river restoration projects in European large rivers (i.e., Rhône, Rhine, Danube, etc.), which sometimes exceed levels outlined in sediment quality guidelines (Middlekoop, 2000; Woitke et al., 2003; Meybeck et al., 2007; Bird et al., 2010), compromising river ecology and human health. The literature provides detailed examples of bed changes observed in large rivers (Phillips, 2003; Habersack and Piégay, 2007; Goshal et al., 2010; Downs et al., 2013; Arnaud et al., 2015). However, alluvial plain responses to such changes in a multi-driver context have rarely been studied, even if they are among the most altered and threatened environments (Tockner and Stanford, 2002). Table 1 shows a selection of works analysing river responses associated with multiple drivers of change. In these works causal factors are often well identified, however, most of them assess the impacts as cumulative river responses, and the single effects of each are not well discerned or hierarchized. Moreover, when examining large rivers, studies frequently focus on a limited section, and few studies examine longer reaches, which allow one to conduct comparative analyses useful for detecting differences and similarities between reaches and for identifying main drivers by deduction. The identification of main drivers of channel change is crucial for river managers to implement successful restoration strategies (Downs and Piégay, 2019).

Table 1

In this work the river-floodplain responses associated with main drivers of change have been evaluated in a large river. Like most of Europe's large rivers, the Rhône River has an extensive legacy of human impact. Engineering work began in the mid-nineteenth century (Poinsart, 1992; Bravard and Gaydou, 2015) with the systematic narrowing and deepening of

groyne fields combined with longitudinal structures for improving navigation. This continued into the second half of the twentieth century when flow regulation was applied for hydroelectric generation purposes (Bravard and Gaydou, 2015). The Rhône River was corrected and its historical course was bypassed with a series of 17 run-of the-river dams from Lake Geneva to the Camargue Delta. In this context, the Rhône River provides a great framework to study river responses associated with different drivers of change.

The objective of this work is to assess the individual effects of the two phases of river modification (channel correction and flow diversion) on floodplain terrestrialisation and connectivity, and evaluate the river response to those phases across time and space. Understanding terrestrialisation as the process affecting the channel-margin aquatic terrestrial transition zone (ATTZ; Junk et al., 1989; Tracy-Smith et al., 2012) whereby pioneer communities invade the former aquatic zone (mainly lentic features) as a result of dewatering or sedimentation, favouring floodplain development.

The approach is comparatively applied to three bypassed reaches that have been subjected to similar human impacts and we use potential controlling factors to separate respective effects of the two regulation phases with potential reach replications (Downs and Piégay, 2019). Moreover, the three sites show clear differences in the chronology of such impacts as well as distinct characteristics. Different fine sediment fluxes and geochemical backgrounds have been identified in the Rhône River by Depret et al. (2017) and Citterio and Piégay (2009), who find higher levels of sedimentation in former channels of downstream reaches that have developed because of higher suspended sedimentation fluxes originating from the Isère Tributary. Such a comparison of reaches should be useful for determining how local features to can used to explain differences in terrestrialisation processes. The understanding of spatial and temporal changes of the natural river–floodplain system induced by river correction and hydropower plant construction is essential for present and future environmental management strategies in the Rhône River, or in other rivers impacted by several drivers of change.

2. Study area

The Rhône River is one of the largest rivers in Western Europe and the most important within the Mediterranean Basin after the Nile River. The Rhône River Basin is the third largest in France, draining a total area of 98,500 km^2 (90,500 km^2 in France). Altitudes in the basin vary from 4800 m in the Mont Blanc Massif to sea level in the Camargue Delta (Fig. 1A). The mean annual discharge level at the gauging station farthest downstream (Beaucaire) is 1720 $m^3\ s^{-1}$ (Olivier et al., 2009). The highest flows recently recorded were in December 2003, when the flow was 12,000 $m^3\ s^{-1}$ in Beaucaire while the 100 yr flood (i.e., Q_{100}) generated a level of 10,300 $m^3\ s^{-1}$ (Provansal et al., 2014), and the highest level recorded was estimated at 13,000 $m^3\ s^{-1}$ during the historic 1840 flood (Bravard, 2010).

From a geological point of view, the Rhône basin is highly variable (the Rhône traverses three mountain ranges – the Alps, the Jura, and the Massif Central), with several major and widely differing tributaries (e.g., Ain, Saône, Isère, Ardèche, Durance), and a valley partially covered by glaciers during the last glaciation periods (the Riss and the Würm). It results in a heterogeneous system characterised by alternating reaches of fixed and mobile channel beds, incised valleys and wide floodplains, and highly distinct sediment inputs (Bravard, 2010).

Over the last two centuries, the Rhône has been heavily modified. Channel modifications began in the second half of the eighteenth century with the construction of longitudinal unsubmersible dykes to protect the population from flooding (Fruget, 1992; Guerrin, 2015). River training continued through the second half of the nineteenth century with the first major development phase, with the channel correction. Such correction is based on a set of modifications such as the construction of groyne fields with each groyne connected to the others by submersible dykes almost continuous from Lyon to Arles, the formation of engineered channel margins referred to as 'Casiers Girardon' and the disconnection of the secondary channels. These infrastructures were built to concentrate flows into a narrow

158 single-bed channel and to promote navigation (Fruget, 1992). The structures constrained
159 fluvial dynamics, favouring rapid morphological changes (Roditis and Pont, 1993; Parrot et al.,
160 2015).

161 During the middle and second half of the twentieth century, the National Company of the
162 Rhône River (CNR), which controls the Rhône River's development, constructed numerous
163 dams (19 in France between the Lake of Geneva and Mediterranean Sea), 17 of which follow
164 the historical river course towards a parallel canal for hydroelectric production. The historical
165 course only receives a very small residual flow (between 30 and 150 $m^3 s^{-1}$), which increases
166 during flood flows, accommodating discharge levels exceeding the maximum operating flows
167 of the plant. Currently, hydropower schemes of the Rhône River account for approximately
168 25% of national hydropower production (Riquier, 2015).

169 Figure 1

170 In this study, three of the bypassed reaches located in the middle reaches of the Rhône have
171 been examined: Pierre-Bénite (PBN), Péage-de-Roussillon (PDR) and Donzère-Mondragon
172 (DZM). They differ in terms of dates of hydroelectric development (PBN, 1966; PDR, 1977;
173 DZM, 1952), bypassed reach lengths (PBN, 11.2 km; PDR, 15.7 km; DZM, 28 km), and maximum
174 levels of discharge processed (PBN, 1380; PDR, 1600; DZM, 1970 $m^3 s^{-1}$; mean discharge levels
175 of the same reaches were valued at 1035, 1060 and 1500 $m^3 s^{-1}$, respectively). We find that
176 PBN, PDR and DZM now represent 57, 50 and 50% respectively of natural 2 yr flooding (Q_2) and
177 73, 69 and 71% of 10 yr flooding (Q_{10}), showing that they are slightly differently affected by
178 peak flow decline (Vázquez-Tarrío et al., 2019).

179 Parrot (2015) also showed that channel incision and armouring occurred within this reach
180 following the first engineering phase. PBN was affected most, experiencing a remarkable
181 incision of 5 m compared to those observed for PDR and DZM of 2.5 m and 1.8 m, respectively.

182 ## 3. Materials and Methods

3.1 Floodplain evolution

To examine planform evolution, two sources of information were used: (i) old maps showing the first stages of river engineering projects (i.e., ca. 1810, 1860, 1905; scale = 1/10,000) and (ii) aerial photographs (for 1938 to 2009; scale = 1/15,000–1/30,000).

The three sets of historical maps used for this work include: (a) a cadastral map (1812-1827) also referred to as the Napoleonic cadastre, (b) a topographical map of the course of the Rhône River dating to 1857-1876 (referred to as the '1860 Atlas'), and (c) a so-called Branciard cartographic map for approximately 1905. The Napoleonic cadastre is a unique and centralized land cadastre established in France under the law of September 15, 1807 from the "cadastre type" defined in 1802. Even though it was not conceived for physical studies (it was the first legal and fiscal tool to impose land taxes on citizens equitably), it has been used for the historical study of land uses and reservoirs (Girel et al. 2003, Poirier, 2006; Lespez et al., 2005; Bartout, 2011). The map serves as a reference of fluvial geomorphologic and landuse conditions present prior to the development of principal river management measures. When we faced doubts concerning the continuity of a paleochannel from one panel to another in the Napoleonic cadastre (sometimes 15 yr apart), we superimposed the Lidar image to ensure their spatial continuity. The 1860 Atlas was drawn by public administration Ponts et Chaussées ('Bridges and Roads'). The map provides a reference of early engineering structures, of their types and of their dates of construction. Finally, the Branciard map offers a relatively complete account of the final phases of engineering structures (Räpple, 2018).

Aerial photos are freely available from the National Institute of Geographic and Forest Information website (IGN-Geoportail).

Historical maps and aerial photographs were georeferenced based on the most recent orthophoto (i.e., 2008) and land registry using ArcMap™ 10.3 GIS. Each map and photo was georeferenced using 15 to 40 control points depending on image sizes. Following the literature

208 (Hughes et al., 2006; Vericat et al., 2008), a second order polynomial transformation model
209 was used and the RMSE associated with georeferenced images ranged from 0.5 to 5 m.

210 The channel planform was digitized from maps and aerial photographs (Figs. 1B and 2) using
211 ArcMap™ 10.3 GIS. We distinguished each available date and active channel, combining flow
212 channels with unvegetated bars (Piégay et al. 2009). The limits of the active channel were clear
213 in the absence of woody riparian vegetation; however, these limits were more ambiguous in
214 the presence of woody vegetation because of the presence of canopy overhangs. In these
215 cases, limits were drawn 4 to 8 m from the edge of vegetation while considering existing gaps
216 between crowns (Liébault and Piégay, 2002). The maps and most of the photos were surveyed
217 for low-flow conditions. Depending on their quality, active channels were digitized at scales of
218 1:500 to 1:1500. Periods used for the floodplain evolution analysis of each site are shown in
219 Fig. 2 and Table 2.

220 Figure 2

221 Once we defined the active channel, maps of morphological changes were created by
222 comparing polygons drawn in each series for the different periods. The comparison of channel
223 positions through time allowed us to create a floodplain map for different time periods
224 corresponding to the start of terrestrialisation and vegetation encroachment (e.g., the
225 disconnection period where time t = the active channel and where t+x = floodplain
226 vegetation). With these maps we assessed geomorphic evolution by comparing variations in
227 active channel widths and the number of flowing channels between different reaches and
228 periods and along each reach. The cumulative active channel width was calculated as the
229 cumulative sum of channel widths taken at 100 m intervals. The cumulative number of flowing
230 channels was calculated as the cumulative sum for the channels at 100 m intervals.

231 The sampling of overbank sedimentation characterization was then based on the obtained
232 maps, allowing us to associate overbank sediment thicknesses or trace metal concentrations
233 with a terrestrialisation period.

234 **3.2 Historical overbank sedimentation**

235 Several field campaigns were carried out to characterize overbank fine sediment deposits. In
236 these campaigns, the thickness of fine sediments overlying gravel deposits was measured. In
237 total, 2366 punctual probes were applied in the three studied reaches: 619 at PBN, 1152 at
238 PDR, and 595 at DZM. Figure 1D illustrates our work on PDR. For probing, a 6 m metal rod with
239 a diameter of 1 cm was used (PANDA Dynamic Cone Penetrometer). Because of the length of
240 the study reaches, we could not sample everywhere, so we created several transversal
241 sections and a sample point was located in the middle of each sedimentation period traversed
242 by the transversal section. Sampling locations were determined based on GIS results to sample
243 all of the sedimentation periods (i.e., the active channel zone for each period). The positioning
244 of each sample was recorded by GPS (Trimble GeoXH, decimetric precision) for subsequent
245 geomatic processing. Table 2 presents the number of samples corresponding to each
246 sedimentation period. It should be noted that sedimentation periods to study floodplain
247 evolution are not exactly the same because the date of the last aerial images range from 2007
248 to 2009 and the fieldwork took place between 2016 and 2017.

249 The fine sediment thickness was defined as the distance between the surface and gravel
250 layer. The depth to gravel was estimated with a rod until it hit gravel following the works of
251 Dufour et al. (2007) and Piégay et al. (2008). This gravel-overbank fine sediment contact is
252 usually fairly clear, notably in such environments where disconnection has been abrupt and
253 good confidence is then observed within GPR measurements and coring evidence (Vauclin et
254 al. 2019). From the ratio of the thickness of fine sediments to the period since floodplain
255 formation (Section 3.1), it is possible to estimate average overbank sedimentation rates

256 (Arnaud et al., 2015; Dufour et al., 2007; Piégay et al., 2008). By using this method, we assume
257 there are no real scouring processes but more surely sediment accretion because of the severe
258 disconnection (see again Vauclin et al. 2019). During field campaigns, scouring processes were
259 only observed in the dike field, much closer features to the main flow channel than the
260 disconnected former channels and floodplains. The period since floodplain formation is
261 determined via photo-interpretation characterized as the water or gravel bare ground surface
262 of year n vegetated in year n + x. The mean sedimentation rate is based on the date of the
263 encroachment period for the centre of floodplain vegetation.

264 Figure 3

265 To calculate sedimentation rates for periods preceding to the earliest date surveyed, we use
266 the age of hydraulic structures (obtained from the 1860 Atlas, see Section 3.1) that have
267 disconnected the main channel, as this marked the start of the sedimentation process.

268 **3.3 Trace elements in floodplain surface sediments as an indicator of connectivity**

269 To use temporal patterns of the superficial metal content of river floodplains as an indicator
270 of connectivity, we must have developed a clear understanding of patterns of contamination
271 flux occurring within a system over a given period. In the Rhône River, peak pollution levels
272 were reached in 1970 (Desmet et al., 2012; Thorel et al., 2018), which decreased
273 systematically after the application of regulations in France in 1975 (Journal Officiel, 1975).
274 Thorel et al. (2018) and Vauclin et al. (2019) already observed this pattern, in which metal
275 elements reached maximum peak during the 1970s before decreasing thereafter. It means
276 that depending on flooding frequency, different floodplain surface sediments should have
277 recorded different patterns of trace elements. Thus, surficial trace elements can be then
278 potentially proxies of floodplain responses to channel changes and connectivity.

279 In total, 749 surface sediments were sampled with a manual auger in the three sections
280 (n=317 in PBN, n=166 in PDR and n=266 in DZM). The sampling design applied was based on

281 cross sections with a series of points randomly distributed across each floodplain vegetation
282 encroachment period. Samples were collected from the surface to 10 to 15 cm in depth (to
283 take into account potential vertical redistribution and homogenization by bioturbation
284 processes) from representative plots of the studied areas (Fig. 1). In total, 100 g of sediment
285 was packaged in plastic bags, identified, located by GPS and immediately transported to the
286 laboratory for analysis. Table 2 shows the number of metal rod probes and surface sediment
287 samples corresponding to each floodplain vegetation encroachment period. The evolution of
288 metal concentrations contained in surficial floodplain sediments by floodplain vegetation
289 encroachment period was determined based on these samples.

290 In the lab, the samples were homogenized to obtain a composite sample of surface
291 sediments. The samples were then dried at 50° C for 72 h, ground with an agate mortar and
292 sieved through a 63 µm stainless steel sieve (Margui et al., 2012; Rouillon and Tailor, 2016).
293 Approximately 10 g of the 63 µm fraction was then placed in XRF sample cups and covered
294 with an X-ray film for analysis. The samples were then analysed using a Spectro® Xsort
295 portable X-ray fluorescence (pXRF) spectrometer housed in a docking station for stationary
296 operation. Via the "Enviro-H" function, the instrument screened for more than 40 major and
297 minor elements in the matrix. Each sample was analysed for 1 min in triplicate to obtain an
298 average for these three measures. This method has been extensively used in previous works
299 (Carr et al., 2006; Melquiades and Appoloni, 2004; Rouillon and Tailor, 2016; Young et al.,
300 2016).

301 Table 2

302 A set of 30 surface samples collected from PBN, PDR and DZM representative of levels
303 identified by pXRF was also analysed with an ICP-MS after *aqua regia* digestion for validation.
304 Correlations between the pXRF and ICP-MS measures are fairly strong (r^2 values of 0.78 to
305 0.94; Fig. 4) for zinc (Zn), lead (Pb), nickel (Ni), and copper (Cu), confirming we can use such

306 low cost pXRF measures to estimate these metal contents over a large set of samples collected
307 within the three reaches.

308 Figure 4

309 **3.4 Vertical channel evolution and lateral connectivity**

310 We used data provided by Džubáková et al. (2015) to assess hydrological lateral
311 connectivity, and we compared these values with overbank fine sedimentation and surficial
312 metal content patterns.

313 These data are based on a LiDAR survey carried out in 2010 by the Institut National de
314 l'Information Géographique et Forestière (IGN) over the Rhône River's full length. The airborne
315 LiDAR DEM was provided in GRID format with a 2 m resolution and an expected accuracy level
316 of 0.2 m in the vertical dimension. The density of the collected pulses was measured as 1-2 m^{-2}
317 where each pulse represents a disc with a diameter of 0.4 m (IGN, 2010). The *Compagnie*
318 *Nationale du Rhône* (CNR) provided daily discharge series for the period 1986–2010 and
319 discharges associated to a 10-yr flood from their gauging stations located in the bypassed
320 sections. Then a relation was established between the discharges and water levels in sections
321 located every 0.6 to 1 km by CNR. The mean standard deviation of data fitting was less than
322 0.17 m in all study reaches, having the greatest deviation at lower flows (<500 m3 s^{-1}),
323 discharges of little interest in this study.

324 Spatial and temporal patterns of lateral connectivity were assessed using a simple, raster-
325 based method, developed in MATLAB and C++ environments. The procedure requires a DEM,
326 rating curves, and flow time series to calculate relative altitude, overflow discharge, flood
327 frequency, and flood duration for a period determined by the flow time series. The method
328 projects the water levels derived from the rating curves into the floodplain to compute
329 overflow discharge and its attributes, assuming that the water level is constant in each of the

cross sections and gradually decreases in the downstream direction (Dzubakova et al., 2015). An example of data obtained for Péage-de-Roussillon can be seen in Fig. 1C.

This method is based in recent hydrological data (1986-2011) and does not allow us to assess hydrological changes over time. A recent work by Vázquez-Tarrío et al. (2016) however, has shown that the frequency of overbank flows in bypassed reaches experienced an important reduction. For instance, the average number of days per year with discharges close to annual flows (1000-2000 m^3s^{-1}) in the bypassed channels decreased from approximately 40-130 to 1-10 d yr^{-1}. Flow discharges corresponding with return periods of 2, 10 and 50 yr have been reduced on average 48%, 62% and 69% after the channel bypass.

We subtracted the overbank fine sediment thickness to the relative floodplain elevation above the channel talweg provided by IGN LiDAR combined with 500 m spacing channel cross sections of CNR to calculate the gravel top elevation. This measure is used to determine previous channel altitudinal positions for each floodplain vegetation encroachment period and to conduct a rough assessment of the vertical evolution of a channel through time. Then, for each sampling point we calculated its present flooding frequency (the number of days per year based on the 1986-2010 flow series) from the map established by Dzubakova et al. (2015).

4. Results

4.1 Channel-planform evolution

The geospatial analysis performed in the three studied reaches (PBN, PDR and DZM) shows that substantial spatial variations have occurred over the last two centuries. During this period, mean active channel widths and surface areas were reduced by almost two thirds in each reach (PBN: 62%, PDR: 59.3%, and DZM: 65.5%, Fig. 5).

Figure 5

353 Declining percentages observed for the active channel surface area show that the two main
354 phases of channel regulation (dike systems and channel bypassing) have a slightly different
355 impact on surface decline within each reach: 40% of the initial surface for the first phase (river
356 engineering, Girardon) relative to 20% for the second (channel bypassing for river power
357 generation), resulting in a 60% cumulative loss of the active channel surface. This pattern of
358 temporal evolution is observed on each of the three reaches.

359 The maximum number of flowing channels in PBN, PDR and DZM measured in 1860 are
360 three, four and five, respectively. In DZM, this is observed in the upper part of its reaches.
361 While DZM was locally braided, PDR and PBN were more anabranched with two to three main
362 flow channels with vegetated islands. In the studied reaches we observed a slight decline in
363 the number of flowing channels that was much more significant for DZM and PDR than for
364 PBN. The mean number of flow channels declined from 2.3-1.7 to 1 flow channels per section,
365 which is fully attributed to the first development phase (Fig. 6). In the second phase, major
366 planimetric changes were mainly related to active channel narrowing in mainly remnant
367 channels and the progressive terrestrialisation and vegetation encroachment of secondary
368 disconnected channels.

369 Figure 6

370 Figure 7 shows that the river has experienced considerable planimetric changes over the last
371 two centuries. A decline in cumulative active channel widths is observed over the studied
372 period across all of the reaches. Cumulative active channel widths normally decreased over
373 time from one date to the next, revealing the effects of the two regulation phases (the
374 Girardon dike system and dam) except for PBN in the year 1993, during which values were
375 slightly higher than they were in 2008.

376 Changes in slope observed among the different curves (years) highlight the most heavily
377 affected sub-reaches of every section (Fig. 7). For instance, steep slopes observed in the

earliest periods covering 8-11 km in PBN, over 54-56 km in PDR, and over 172-178 km in DZM reveal the presence of wider sections compared to those of the other periods. For these same reaches, slopes are much lower and more constant in the most recent periods, demonstrating a trend of significant narrowing. We do not find any changes from upstream to downstream areas, which is related to bedload starvation. A progressive narrowing of the widest sections over time is mainly related to the two periods of development identified above. While active channel widths were fairly variable longitudinally from the start to the middle of the nineteenth century, they have become highly homogeneous after the two phases of regulation.

Figure 7

The cumulative number of flowing channels per 100-m-long segment follows the same pattern as that followed by active channel widths with a decline observed over time. Rather than the progressive decrease of cumulative active channel widths, this value mainly appears to be impacted by the Girardon dyke system phase, after which all local anabranching reaches evolved into single thread channels.

Overall, the changes observed for the last two centuries are significantly related to the two development phases. The first mainly shaped the flow concentrations of single-bed channels with most channels narrowing, whereas the second only affected narrowing.

4.2 Floodplain terrestrialisation

Two main factors influence patterns and levels of floodplain terrestrialisation and lateral disconnection from the main channel overflow. River incision seems to be an important factor as well as overbank fine sedimentation with the second factor also being controlled by incision.

In the three studied areas of the Rhône River, the impact of river incision on overbank deposition occurring in response to channel regulation involves a progressive decline in gravel

top elevation according to the period of floodplain establishment (see Fig. 1C and Section 3.2). From Fig. 8A, we can distinguish between different patterns of incision for the three studied reaches. In PBN, the older surfaces terrestrialised early on, the relative height of the gravel surface is the most elevated; however, after the Girardon embankment, a very clear period of incision affected the oldest surfaces ~ 3.6 m (1860-1905) to 0.5 m (2008-2016) above the talweg. The data show a large volume of coarse sediment in PBN of nearly two times greater than that observed in PDR. PDR and DZM suffer from a slighter incision and the effect of the Girardon phase is not as critical. The DZM gravel layer is thicker than that observed in PDR. In both cases, a small amount of incision developed during the period with local anomalies occurring in the most recent period in DZM and in periods immediately preceding and following the dam's completion with PDR trends.

Figure 8

An overall reduction in fine overbank sediment thicknesses and sedimentation rates in the three sections is reported for the twentieth century (Fig. 8B and C). We cannot differentiate classical progressive reductions in sedimentation rates of old units from recent ones. When considering reference values calculated for the period preceding the Girardon construction, a maximum value of fine sedimentation is observed immediately after the Girardon construction for PBN and DZM. In PDR, the highest level of fine sedimentation occurs immediately before Girardon.

The completion of the Girardon structures has therefore had a clear impact on overbank sedimentation (Fig. 8B). After the Girardon phase, in PBN and DZM, a fairly high fine overbank sediment thickness is observed until the bypassing phase in contrast with patterns observed for PDR, which undergoes a decline earlier on. The effects of channel bypassing are common in the three sections, though decreasing trends become more evident some years after the river's regulation.

428 The median thickness of PBN fine sediments is the lowest of the three sections with a
429 median value of 1.2 m, registering a maximum immediately after the Girardon embankment
430 phase (1.25 m). The values recorded for PDR and DZM are much higher than those recorded
431 for PBN with median values of 1.8 and 1.7 m, respectively. For PDR, we observe the highest
432 thicknesses of fine sediments for 1860 to 1905 (2.6 m), while in DZM the estimated
433 thicknesses are larger in the newest floodplain (1947-1955).

434 When fine sedimentation rates are analysed as a function of the sedimentation period, the
435 patterns are fairly similar to those observed for overbank sediment thicknesses. For PBN,
436 median sedimentation rates increased from 1860 to a maximum value of 1.7 cm yr^{-1} observed
437 from 1905-1945 (Fig. 8B), after which they decreased. Temporal variations in sedimentation
438 rates observed in PDR contrast with those observed for PBN. In PDR, the highest rates are
439 observed from 1860-1905 (1.9 cm yr^{-1}), and a sharp decline is observed thereafter until values
440 nearly reach zero during the most recent period. Two very steep declines in sedimentation
441 rates are also observed with one occurring after the Girardon construction and with the other
442 occurring after bypassing. The pattern observed for DZM is quite similar to that observed for
443 PBN, although it is less marked with an increase in sedimentation rates occurring until the
444 1947-1955 sedimentation period and then with a decrease occurring in the most recent
445 periods. Again, in DZM and PBN, one of the most pronounced changes in sedimentation rates
446 is observed immediately after bypassing.

447 It is interesting to investigate fine sedimentation patterns in detail using, in addition to
448 terrestrialisation periods, different floodplain compartments. When we analyse overbank
449 sedimentation patterns of the two main floodplain compartments disconnected in the
450 twentieth century (e.g., Girardon casiers and disconnected former channels), we observe
451 different trends from one section to the other. For instance, for PBN we find a very significant
452 sedimentation pattern in the Girardon casiers relative to disconnected former channels. In PDR
453 the sedimentation pattern is slightly reversed, accounting for very pronounced patterns of

454 sedimentation in disconnected channels (distal floodplain) observed at the start of the period
455 relative to the casiers (proximal floodplain). Downstream in DZM we find no clear differences
456 between the sedimentation patterns of both floodplain compartments.

457 Figure 9

458 **4.3 Trace elements in floodplain surface sediment**

459 A wide range of metal concentrations is observed in the surface sediment of the floodplain.
460 Average and standard deviations of trace element concentrations in the PBN samples are
461 higher than those found for samples taken from PDR and DZM (Table 3).

462 Concentrations of Zn and Cu were found to be higher in the PBN and PDR sections with
463 several extreme values observed in the higher quantile. In contrast, we found higher levels of
464 Ni in DZM, suggesting that the two upstream sections indeed present a different chemical
465 signature from those of the downstream section.

466

467 Table 3

468 When patterns of trace element concentrations are displayed as a function of the
469 vegetation encroachment period, they are clearly different among sites (Fig. 10). In general,
470 concentrations of the studied elements are relatively higher in floodplain surface sediments
471 that started to be settled immediately after completion of the Girardon structure. During the
472 reference period (1810-1860), all elements show high concentrations and then undergo
473 gradual and irregular patterns of decay until the 2000s. We observed a decline in the
474 concentrations of all elements as the period of floodplain vegetation encroachment was
475 shortened, with patterns being less pronounced in the case of Ni.

476 Figure 10

477 The observed trends are slightly different for each of the three sections. In PBN,
478 concentrations increase slightly from 1905-1945, after which concentrations decline gradually

to the 1993-2008 terrestrialisation period. Finally, a clear increase is observed for deposits representing the most recent period; however, it should be noted that the values are based on a single sample.

Chemical levels underwent a clear decline to the 1950s in PDR followed by a slight increase in more recent deposits of Cu and Pb. Levels of inter-period and inter-sample variability are much lower for PDR than for PBN. In PDR the highest concentrations of Zn occur after the 1950s.

In DZM, metal concentrations increase to the 1947-1955 terrestrialisation period and progressively decrease on younger surfaces. We observe an exception in the case of Ni, for which we find an abrupt increase in concentrations for the most recent period with median values exceeding those observed in the reference period.

4.4 Channel planform evolution, connectivity and superficial metal content

The presented connection frequency is analysed comparatively among the reaches as a potential proxy of differences in processes governing floodplain formation and evolution.

Figure 11

Figure 11 shows clear differences in terms of present levels of floodplain surface connectivity by period of terrestrialisation, and patterns are also very different from one reach to another. DZM, given the higher relative elevation of most of its surfaces, is the most disconnected reach because of the combined effects of incision and overbank sedimentation. Even fairly new terrestrialised surfaces record significant gravel thicknesses. As is shown above, PBN is the reach that was most affected by channel incision in earlier terrestrialisation periods, constituting the main source of channel-floodplain disconnection. In this reach, the oldest surfaces of high elevation are very disconnected while newer surfaces are more connected than those in DZM and as connected as those in PDR. This latter findings explains the higher sedimentation rates observed in the newest areas relative to the other sites. PDR is

504 the more connected reach; disconnection has mainly been governed by overbank
505 sedimentation rather than by channel incision.

506 The relations between present connectivity and other geomorphic variables such as
507 floodplain elevation, gravel thickness, fine sediment thickness and sedimentation rates were
508 explored to better understand the floodplain's evolution. We generally find an inverse linear
509 relationship with the present connection frequency regardless of the reach and geomorphic
510 variables considered. When analysing the relation between floodplain elevation and flooding
511 frequency (Fig. 12A), the floodplain elevation of PDR is lower than those of the two other
512 sections, revealing differences between the reaches in terms of hydraulic geometry, but with
513 no clear downstream pattern. The slope of the relationship between floodplain elevation and
514 flooding frequency is also similar regardless of the reach considered. In DZM, the floodplain
515 elevation of older surfaces is the same as that observed for PBN; DZM differs from the other
516 reaches in that here the newest surfaces are positioned more than 1 m higher than the other
517 reaches and possibly as a consequence of overbank fine deposition.

518 Figure 12

519 Sediment thicknesses and rates (Fig. 12C and D) respond differently to connection
520 frequencies depending on the reach considered. While in DZM the reaction to a decline in
521 connection frequency involves a significant decrease in sediment thickness and sedimentation
522 rates, for PBN the reduction is less important, and PDR occupies an intermediate state.
523 Overbank sedimentation effects on DZM disconnection are remarkable and less marked for
524 PBN. Disconnection in PBN is mainly related to channel incision and associated floodplain
525 gravel thickness and not to overbank fine sedimentation.

526 The metal concentrations in floodplain surfaces are also affected by the frequency of
527 overbank flows. For sedimentation rates and sediment thickness, an inverse relation exists
528 between the connection frequency and metal concentrations with the only exception found

529 for Ni and Cu in DZM (Figs. 13A and B). The slope of trend lines for this section is quite variable.
530 For PBN and PDR the regression slope is similar, and the lines are largely parallel, following the
531 same patterns observed in response to an increase in connection frequency.

532 Figure 13

533 ## 5. Discussion

534 ### 5.1 Changes related to the two regulation phases

535 #### 5.1.1 Narrowing

536 In the existing literature, channel adjustment processes have mainly been studied
537 individually. Many works have described channel adjustments made to rivers below dams
538 (Petts, 1984; Kondolf, 1997; Phillips, 2003; Batalla et al., 2006), while fewer have examined
539 lateral in-channel hydraulic structures (Surian and Rinaldi, 2003), and studies have rarely
540 focused on both types of human pressure simultaneously (Hohensinner et al., 2004). The
541 present work serves as a study of the latter where the impacts of two different types of
542 channel pressure have been assessed separately to assess whether their effects are cumulative
543 or counteract one another.

544 In the study period (i.e., 1810 and 2010), channel narrowing is observed in the three
545 sections and is slightly more marked in DZM (66%) than in PDR (60%). These values reflect
546 channel reductions of 0.45, 0.42, and 0.41% yr^{-1} in DZM, PBN and PDR, respectively. From
547 these percentages, approximately 40% of the initial surface retraction is associated with the
548 first phase (groyne and dike systems and Girardon construction), while 20% is associated with
549 the second phase (channel bypassing for river power generation). Values obtained in the first
550 phase vary from 0.38 to 0.55% yr^{-1}. However, the decline in the width of the Rhône River in the
551 second phase becomes more relevant when we take into account the short time period over
552 which this reduction took place, registering values of 0.57 to 0.80% yr^{-1}. This trend is then fairly

553 comparable from one reach to the other even if slightly different chronologies are found for
554 each of the reaches, confirming the systematic effects of each type of human pressure.

555 When comparing the values observed to those obtained for other rivers affected by
556 damming and other in-channel human-induced impacts such river embankment and
557 channelization, channel narrowing processes of the Rhône River are far from reaching
558 maximum values obtained in past studies. It can be said that these values are the average
559 values of their European counterparts. For instance, Hohensinner et al. (2004) have shown a
560 cumulative reduction in the average channel width of the Danube River of approximately 60%
561 from 1826 to 1991, echoing the values found for the Rhône. Channel reductions observed each
562 year varied from 0.46% (after massive embankments) to 0.26% after channelization and dam
563 construction, and this latter value is lower than that observed for the Rhône and perhaps
564 because of the smaller impact of dams on the decline of peak flows on the Danube River.
565 Arnaud et al. (2015) showed the rapid response of the Rhine River to the completion of the
566 bypassing scheme in the 1950s, exhibiting 26% channel narrowing over 40 yr (0.65% yr^{-1}) and
567 again echoing the values presented here. For the Piave River (Italy), the combination of several
568 human impacts (streambank protection structures, gravel mining, flow diversion, river
569 regulation, etc.) led to channel reductions of between 58 and 70% over 97 yr (ca. 0.63% yr^{-1};
570 Surian 1999). For the Rhône River, most narrowing occurred in the Girardon phase without any
571 change in the peak flow. In this case, structures altered hydraulic conditions in two ways: (i) by
572 increasing levels of shear stress acting on narrow channels, by increasing transport capacities
573 and sometimes by incision when sediment supplies did not increase in kind and (ii) by reducing
574 the flow magnitude of engineered margins and by maximizing overbank fine sedimentation,
575 terrestrialisation and associated vegetation encroachment. The second phase is mainly related
576 to a change in peak flow as shown by Vázquez-Tarrío et al. (2018), and as observed by Arnaud
577 et al. (2015), for the Rhine. It is less significant than the first period, during which only
578 hydraulic changes occur, and these changes are not as significant as what is observed

downstream from large reservoirs where declines of peak flows can be very impactful. In the Platte River, the channel width at the Brady station changed from 1250 to 45 m between 1865 and 1969, representing a decline of 96.4% occurring over 104 yr (i.e., 0.93% yr^{-1}; Williams, 1978). This case can be deemed extreme given the dramatic impact of dams in reducing peak flows. Narrowing is usually linked to peak flow decline, and according to stations along the Platte River with pre-dam records, the reduction of average peak flows is recorded at approximately 90%.

Common trends can be observed for the three reaches for the 1810–2010 period. For the general trend of active channel narrowing, we can identify cycles of reaction-relaxation times following human disturbance. A significant narrowing of the active channel was recorded during the first half of the twentieth century. Intense channel narrowing recorded between 1905 and 1950 (roughly 30%) corresponded to (i.e., 45 yr) the Rhône River rapidly responding to alluvial plain disconnection generated by the Girardon structures. The river then experienced a relaxation period to reach a new steady state (visible at PBN and PDR), as active channel widths were stable before the commissioning of diversion dams (Fig. 5). A second reaction time period is observed after the commissioning of diversion dams where roughly 10-20% of the active channel zone declined depending on the river section. For instance, in PBN this intense response took place over ten years, a period of time similar to that observed by Arnaud et al. (2015) for the Rhine of Kembs. For PDR and DZM the reaction time was prolonged. The river then once again underwent surface stabilization and the very progressive decline of its active channel zone, reflective of system stabilization and slow terrestrialisation processes. As is shown for PBN and PDR, initial narrowing may have also occurred before the Girardon construction. This narrowing corresponds to the reaction period of the first embankments (flood protection) occurring at the end of eigtheenth century and in the beginning of the nineteenth century (Fruget, 1992) and to an initial decline in bedload delivery caused by the ending of the Little Ice Age and because of progressive catchment

phytostabilization, mitigating potential effects of important floods such as those occurring in 1840 and 1856 (Olivier et al., 2009). Although we cannot prove that the river reached a steady state (relaxation time), decreasing rates gradually diminished (~10% between 1860 and 1905). This slight stabilization is not observed for DZM because of the lack of data for this period.

5.1.2 Sedimentation

Overbank fine sedimentation is also characterized by two main river training phases.

Higher sedimentation rates appeared following the first training period. The classic trend of decreasing sedimentation rates from young to old units (Nanson and Beach, 1977; Hooke, 1995) is not observed along the Rhône's margins. Older surfaces exhibit more signification sedimentation rates than newer surfaces.

Several factors can explain the decline of sedimentation observed over time. The groyne and dike systems conceived by the Girardon construction exhibit strong capacities to trap suspended sediment in the period immediately after their completion when the studied reaches experienced the highest sedimentation rates (except in DZM, where they decreased slightly). The effects of Girardon structures increased sedimentation rates from 1-1.5 to 2 cm yr^{-1}. The absence of major dams during this period and the different land uses involved (deforestation and higher levels of agricultural activity) explain the higher magnitude of fine sediment fluxes registered until this period. Afterwards, the closure of several dams along the Rhône River and along main tributaries during the first half of the twentieth century (Guertault, 2015; Olivier et al., 2009) and major changes in land use (agricultural abandonment and subsequent afforestation; Liébault and Piégay, 2002; Citterio and Piégay, 2009; Piégay et al., 2004, Buendía et al., 2016, García-Ruiz et al., 1996, García-Ruiz and Lana-Renault, 2011) can explain the reduction in suspended sediment loads transported by the Rhône. In addition, channel bypassing in the studied reaches reduced flood peaks, decreasing the period of time in

630 which the floodplain is inundated and thus the amount of sediment deposited. All of these
631 factors thus contribute to temporal patterns of floodplain sedimentation observed along the
632 Rhône River.

633 Depending on the reach studied, estimated median sedimentation rates vary from 1.2 to 1.8
634 cm yr^{-1}; however, high levels of variability are observed with values ranging from a minimum of
635 0.1 cm yr^{-1} to a maximum of 14 cm yr^{-1}. Observed values, even when affected by exacerbating
636 human effects, are not exceptionally high. For other large European rivers, similar values can
637 be found. For instance, for the Rhine River, Arnaud et al. (2015) registered median rates of
638 overbank sedimentation of between 1.9 and 8.1 cm y^{-1}. In contrast to our data, however, they
639 found the highest sedimentation rates in the newest patches. In the lower parts of the same
640 river, rates ranged from 0.2 to 1.5 cm yr^{-1} (Middlekoop, 2000). Barth et al. (1998) obtained an
641 average sedimentation rate of approximately 3 cm yr^{-1} for the period from 1945 for an
642 embankment near Aken in the Elbe River, and in a more recent study Krüger et al. (2006)
643 calculated sedimentation rates of between 0.2 and 1.5 cm yr^{-1} for locations close to the river.
644 Begy et al. (2015) reported rates for the Danube River very similar those obtained for the Elbe
645 (i.e., 0.1 to 1.8 cm yr^{-1}). For North America, rates mentioned in the literature are usually lower
646 than those obtained for the Rhône River. Average sedimentation rates given by White et al.
647 (2002) for rivers along the Texas coastal plain are much lower than those presented here,
648 ranging from the 0.26 cm yr^{-1} of those of the Nueces system and the 0.5 cm yr^{-1} of those of the
649 Trinity River. Knox (2006) found that 0.02 cm yr^{-1} reasonably approximates the long-term
650 average rate of Holocene vertical accretion in the Upper Mississippi River, while after being
651 influenced by human activities (mainly agriculture) the rates increased to between 0.5 and 0.2
652 cm yr^{-1}. Sedimentation rates estimated by Page et al. (2003) in Murrumbidgee River (Australia)
653 were higher than the observed in North American rivers, showing an average vertical accretion
654 rate of between 1 and 4 cm yr^{-1}.

655 **5.1.3 Metal contents**

Figure 10 shows a general decline in metal content in the floodplain surface with older concentrations being the most affected. This pattern must involve both the chronology of flux and connectivity and associated sedimentation. Brewer and Taylor (1997) noted this same pattern, suggesting that some high flows occurring during mining periods create a blanket of polluted overbank fines in pre-mining non-polluted deposits of the upper Severn Basin. This explains the higher concentrations of metals found in ancient deposits, which may be what we can expect from the Rhône. Its older surfaces, which are only occasionally flooded, present signs of pollution dating to the twentieth century and show a peak occurring in the 1970s, whereas newer surfaces are much more connected with recent sedimentation patterns revealing relatively clean sediment surfaces. For surfaces established in the 1970s and 1960s, contamination may exist but only within sediment compartments. Metal elements has been used as tracers in other studies to report historical high-resolution dating for overbank floodplain vertical accretion (Knox, 2006). Additionally, in this work, we used the metal elements as connectivity proxies. The presence of these elements in surface sediments allows us to clearly differentiate the levels of connection. High metal concentrations related with the flows of the 1970s mark the least connected surfaces, compared to the most frequently connected surfaces that have recorded the less contaminated fluxes of recent decades. These findings complement the results of previous studies of sediment cores (Seignemartin et al., 2018; Thorel et al., 2018; Vauclin et al., submitted; Seignemartin et al., 2019) carried out in the Rhône River.

5.2 Drivers governing inter-reach variability

5.2.1 Channel adjustments

Channel narrowing in the Rhône River does not significantly vary from one reach to another in terms of the intensity of changes and the chronology of adjustments and surfaces

680 concerned. We only observe a chronological shift in channel adjustments related to bypassing
681 that is only linked to the date of dam construction (Fig. 5B).

682 Major variations in channel adjustments are linked to vertical channel reactions to Girardon
683 infrastructures. Whereas PDR showed only a slight incision, PBN was the most heavily incised.
684 This main inter-reach difference is common to long regulated reaches. PBN, which is located in
685 the upper sections with major infrastructure, is subjected to higher levels of shear stress than
686 the other reaches (Vázquez-Tarrío et al., 2019), and an increase in transport capacity not
687 compensated by an increase in upstream bedload delivery because upstream from Lyon, no
688 infrastructures similar to the Girardon have been built to increase transport capacities.
689 Because PBN is the most upstream embanked reach, it has been the most reactive. A
690 progressive propagation of changes from upstream is also observed along the Rhine (Arnaud
691 et al., 2015). For PDR, shear stress levels increased in upstream reaches, increasing bedload
692 supplies and minimizing local impacts on channel depths resulting from human disruption.
693 DZM was subjected to an intermediate situation. Incision occurred to a lesser extent than in
694 PBN because of effects of upstream reaches and tributaries. Disconnection observed in this
695 section can be partly related to a fairly intense period of gravel extraction occurring in the
696 1960s (Marteau, 1993). Hence, we do not find strong relationships between gravel thickness
697 and channel connections as shown for PBN, and the gravel layer in this reach is the thickest of
698 those of the three sites for the newest floodplain surfaces.

699 **5.2.2 Floodplain formation**

700 Floodplain formation or terrestrialisation is a complex process related to channel
701 disconnection occurring because of overbank sedimentation or water level lowering following
702 channel incision or water derivation.

703 Fine overbank sedimentation along floodplains is a very complex process mainly influenced
704 by a difference in elevation (lateral connectivity) between a channel and floodplain, which

controls the frequency, duration, magnitude and suspended sediment concentration (SSC) of floods (Asselman and Middelkoop, 1995; Piégay et al., 2008; Gautier et al., 2009; Harrison et al., 2015) as well as the density of vegetation controlling roughness and trapping efficiency (Gautier et al., 2009; Harrison et al., 2015). In such a context, the degree of river training (Wu et al., 2005) can greatly influence floodplain sedimentation rates mainly because it can affect the topography and associated lateral connectivity (e.g., the frequency and magnitude of overbank flows).

When a river is confined by river-control structures and remains laterally stable, the river usually experiences incision (most notably in its upper section), where sediment delivery is not changed, which is the case for PBN. This process can raise the relative elevation of the floodplain above the riverbed, considerably reducing the frequency of overbank flows and thus sedimentation in the floodplain (Wyzga, 2001). Floodplain formation occurred with the same intensity and chronology along the three reaches, but it is related to two different processes. For PBN, it is mainly linked to channel incision but also to lower levels of overbank sedimentation because it was quickly disconnected. In contrast, for PDR and DZM, early incision did not occur and its reaches are closely connected and have undergone intense periods of overbank sedimentation.

PDR is less incised and thus a more connected section that exhibits slightly varied patterns of sedimentation from the channel to the distal part of the connected floodplain. In this case, rates of distal sedimentation are higher than those observed in proximal areas, which is not the case for PBN (Fig. 9).

It is worth also highlighting the anomalous behaviours of the newest proximal surfaces of PBN (post 1970s). For the same connection frequency level (i.e., 50-60 d yr^{-1}; Fig. 12D), these surfaces register much higher sedimentation rates than those observed in PDR. The proximal location of the Saône-Rhône confluence may serve as an explanation, increasing suspended sediment concentrations flowing into the bypassed reach. The sediment plume transported

731 from the Saône River is not diluted before flowing into PBN with suspended sediment flux
732 being significantly higher than in the other sections (see Fig. 5.8 in Le Coz, 2007).

733 **5.2.3 Metal content**

734 Other factors not related to overbank sedimentation or lateral connectivity may influence
735 metal content levels in the floodplain and may explain the different patterns observed among
736 the three studied reaches. Apart from well-known sources of pollution as an industrial area
737 (industrial waste), for PBN the most polluted samples originate from areas located close to
738 urban regions. One potential source is related to stormwater runoff, which is favoured by
739 impervious surfaces and travels through urban areas, gathering a wide variety of pollutants
740 that are then delivered to the floodplain. Another source is related to the proximity of
741 transportation infrastructures. Railroads and roadways are a significant nonpoint source of
742 pollutants, and even recreation paths into the floodplain have been affected by high
743 concentrations of Pb perhaps caused by illicit car maintenance (oil changes, car washes, etc.).
744 In PDR and DZM, the proximity of urban areas is not as marked as it is in PBN, and floodplains
745 are mostly surrounded by agricultural fields and local industries.

746 Alternatively, we identify a clear longitudinal pattern of metal content in the three studied
747 reaches with a decline observed from the industrialised and urbanised region upstream to the
748 agricultural region downstream. This urbanization gradient affects chemical structures of the
749 different sections with Zn and Cu serving as indicators of river systems located in densely
750 populated and industrialized areas with elements found in higher concentrations in the
751 upstream region (PBN and PDR). In contrast, in the downstream region (DZM), higher Ni levels
752 in the surface sediments can be attributed to the inputs of western tributaries, which flow
753 through volcanic and crystalline bedrock (e.g., the Ardèche and Eyrieux rivers). Moreover,
754 inputs from the less polluted Isère and Drôme rivers found in the reaches following PDR may
755 produce signal dilution effects in DZM.

The differences between PBN and PDR in terms of Cu and Pb levels are important, whereas for Zn and Ni this is not found to be the case. Although these values are surely influenced by the features of urban and industrial pollution sources, studies of the Sena River recognize atmospheric fallout as a major contamination pathway (Thévenot et al., 2007). Observations of air quality levels for the Auvergne-Rhône-Alpes region show that Cu and Pb concentrations are more elevated in the vicinity of Lyon (PBN) than in PDR (ATMO, 2014). This information becomes more relevant when we consider the fact that in our work we analyse pollution in surface sediments, which are more susceptible to contamination from this source of pollution than sediments obtained from greater depths (i.e., core sampling). Atmospheric inputs may be more important than flow inputs and lateral connectivity levels in explaining why older surfaces are characterized by significantly higher Zn and Pb levels than newer surfaces with a clear gradient observed from urban to rural reaches. For newer surfaces, this atmospheric signal is smoothed by overbank sediment originating from sediment sources less influenced by urban areas.

6. Conclusion

The Rhône River has been heavily regulated over the last two centuries. The two phases of channel regulation have affected the three study reaches in the same manner, but not with the same magnitude. During the study period, the impact of both regulation phases resulted in a general narrowing of the studied reaches (i.e., a 60 to 66% loss of active channel width). Nevertheless, our data point to river in-channel hydraulic structures as the primary source of channel planform shrinkage, accounting for 40% of channel narrowing while channel bypassing accounts for the remaining 20%.

Channel narrowing in the Rhône River has initiated other adjustments and mainly those related to incision. Such processes have varied depending on the longitudinal positioning and local characteristics of each studied reach. PBN has been the most heavily incised because of

high levels of shear stress generated by an absence of engineering structures in upstream reaches not being compensated by an increase in sediment delivery upstream. In contrast, in PDR and DZM, incision levels were lower because the incision of the upper modified reaches supplied enough bedload sediment to ensure equilibrium with excess shear stress and to minimize local impacts of these infrastructures.

Spatial and temporal overbank sedimentation patterns are highly variable and complex as a result of the interaction between numerous factors such as topography, flood frequency, connectivity, etc. Channel incision and overbank deposition serve as key controls of hydrological connectivity between floodplains and main channels, and the magnitude of such processes influences the complexity of overbank sedimentation in the floodplain and in different reaches.

Anthropogenic interference has clearly altered natural floodplain sedimentation patterns, and the oldest surfaces do not record the highest sedimentation rates. In this study we found that more connected areas (usually newer surfaces) sometimes register lower sedimentation rates, while the less connected areas register higher sedimentation rates. Metal tracers in the studied floodplain follow the same pattern where highest concentrations were found with a low connection frequency. The heavy metal distribution observed in the Rhône River floodplain is closely related to patterns of sediment deposition; however, other factors such as the background context, the proximity of urban or industrial areas, and atmospheric fallout can modify their distribution and levels.

Understanding local factors controlling floodplain sedimentation and terrestrialisation is therefore necessary for predicting their behaviour in terms of sedimentation and scouring patterns. Such information is critical for informing river managers and for improving restoration plans and the determination of channel reaches to restore.

7. Acknowledgements

This study was conducted as part of the Rhône Sediment Observatory (OSR) program, a multi-partner research program funded through Plan Rhône of the European Regional Development Fund (ERDF), Agence de l'eau Rhône Méditerranée Corse, CNR, EDF and three regional councils (Region Auvergne-Rhône-Alpes, PACA and Occitanie). The work was performed within the framework of the EUR H_2O'Lyon (ANR-17-EURE-0018) of Université de Lyon (UdL) through the "Investissements d'Avenir" program operated by the French National Research Agency (ANR) and through Labex DRIIHM, French programme "Investissements d'Avenir" (ANR-11-LABX-0010) managed by the ANR of the Observatoire Hommes-Milieux Vallée du Rhône (OHM VR). We would like to thank EVS 5600 Laboratory staff Brice Noirot, Jérémie Riquier, Kristell Michel, Massor Hind and Lise Vaudor for their support with the field campaigns and with data treatment and analysis.

818 **References**

819 Allred, T. W., Schmidt. J. C., 1999. Channel narrowing by vertical accretion along the Green
820 River near Green River, Utah. Geological Society of America Bulletin, 111:1

821 Amoros, C. and Bornette, G., 2002. Connectivity and biocomplexity in waterbodies of
822 riverine floodplains. Freshwater Biology 47, 761–776.

823 Arnaud, F., Piégay, H., Schmitt, L., Rollet, A.J., Ferrier, V., Béal, D., 2015. Historical
824 geomorphic analysis (1932–2011) of a by-passed river reach in process-based restoration
825 perspectives: The Old Rhine downstream of the Kembs diversion dam (France, Germany),
826 Geomorphology 236, 163–177.

827 Arnaud, F., Piégay, H., Béal, D., Collery, P., Vaudor, L., and Rollet, A.J., 2017. Monitoring
828 gravel augmentation in a large regulated river and implications for process-based restoration.
829 Earth Surface Processes and Landforms 42, 2147–2166.

830 Asselman, N.E.M. and Middelkoop, H., 1995. Floodplain sedimentation: quantities, patterns
831 and processes. Earth Surface Processes and Landforms 20, 481–499.

832 ATMO (2014) Suivi des niveaux de polluants atmosphériques sur le Pays Roussillonnais en
833 2014 (www.atmo-auvergnerhonealpes.fr)

834 Auble G.T., Friedman, J.M., Scott, M.L., 1994. Relating riparian vegetation to present and
835 future streamflows. Ecological Applications 4(3),544-554.

836 Bartout, P., 2011. L'apport du cadastre napoléonien aux problématiques spatiales des
837 retenues d'eau [archive]. Revue Géographique de l'Est 51(3-4).

838 Batalla, R.J., Vericat, D., Martínez, T.I., 2006. River-channel changes downstream from dams
839 in the lower Ebro River. Zeitschrift für Geomorphologie 143, 1–14.

840 Begy, R.C., Simon, H., Reizer, E., 2015. Efficiency testing of Red Lake protection dam on Rosu
841 stream by 210Pb method. Journal of Radioanalytical and Nuclear Chemistry 303(3), 2539–
842 2545.

843 Bravard, J.P., 2010. Discontinuities in braided patterns: The River Rhône from Geneva to the
844 Camargue delta before river training. Geomorphology 117(3), 219–233.

845 Bravard, P. and Gaydou, P., 2015. Historical Development and Integrated Management of
846 the Rhône River Floodplain, from the Alps to the Camargue Delta, France. In: P.F. Hudson and
847 H. Middelkopp, eds. *Geomorphic Approaches to Integrated Floodplain Management of*
848 *Lowland Fluvial Systems in North America and Europe*. New-York: Springer, 289–320.

849 Buendía, C., Bussi, G., Tuset, J., Vericat, D., Sabater, S., Palau, A., Batalla, R.J., 2016. Effects
850 of afforestation on runoff and sediment load in an upland Mediterranean catchment. Science
851 of the Total Environment 540, 144–157.

852 Brewer, P.A. and Taylor, M.P., 1997. The spatial distribution of heavy metal contaminated
853 sediment across terraced floodplains. Catena 30, 229–249.

854 Cadol, D., Rathburn, S.L., Cooper, D.J., 2010. Aerial photographic analysis of channel
855 narrowing and vegetation expansion in Canyon De Chelly National Monument, Arizona, USA,
856 1935–2004. River Res. Appl. 27, 841–856.

857 Carr, R., Zhang, C., Moles, N., Harder, M., 2008. Identification and mapping of heavy metal
858 pollution in soils of a sports ground in Galway City, Ireland, using a portable XRF analyser and
859 GIS. Environ. Geochem. Health 30, 45–52.

860 Citterio, A. and Piégay, H., 2009. Overbank sedimentation rates in former channel lakes:
861 characterization and control factors. Sedimentology 56, 461–482.

862 Coops, H., Beklioglu, M., Crisman, T. L., 2003. The role of water-level fluctuations in shallow
863 lake ecosystems—Workshop conclusions. Hydrobiologia 506–509, 23–27.

864 Cowx I. G. and Welcomme R. L., 1998. Rehabilitation of rivers for fish, 204pp. Oxford, UK:
865 Fishing News Books, Blackwell Science.

866 David, M., Labenne, A., Carozza, J.-M., & Valette, P., 2016. Evolutionary trajectory of
867 channel planforms in the middle Garonne River (Toulouse, SW France) over a 130-year period:

868 Contribution of mixed multiple factor analysis (MFAmix). Geomorphology 258, 21–39.
869 doi:10.1016/j.geomorph.2016.01.012

870 Depret, T., Riquier, J., Piégay, H., 2017. Evolution of abandoned channels: Insights on
871 controlling factors in a multi-pressure river system. Geomorphology 294, 99–118.

872 Desmet, M., Mourier, B., Mahler, B., Van Metre, P., Roux, G., Persat, H., Lefèvre, I., Peretti,
873 A., Chapron, E., Simonneau, A., Miège, C., Babut, M., 2012. Spatial and temporal trends in PCBs
874 in sediment along the Lower Rhône River, France. Science of the Total Environment 433, 189–
875 197

876 Downs, P.W., Dusterhoff, S.R., Sears, W.A., 2013. Reach-scale channel sensitivity to multiple
877 human activities and natural events: lower Santa Clara River, California, USA. Geomorphology
878 189, 121–134.

879 Downs, P.W., Piégay, H., 2019. Catchment-scale cumulative impact of human activities on
880 river channels in the late Anthropocene: implications, analytical limitations and prospect.
881 Geomorphology 338, 88–104

882 Dufour, S., Barsoum, N., Muller, E., Piégay, H., 2007. Effects of channel confinement on
883 pioneer woody vegetation structure, composition and diversity along the River Drôme (SE
884 France). Earth Surf. Process. Landf. 32, 1244–1256.

885 Dynesius, M., Nilsson, C., 1994. Fragmentation and Flow Regulation of River Systems in the
886 Northern Third of the World. Science 266 (5186), 753-762.

887 Džubáková, K., Piégay, H., Riquier, J., Trizna, M., 2015. Multi-scale assessment of overflow-
888 driven lateral connectivity in floodplain and backwater channels using LiDAR imagery.
889 Hydrological Processes 29, 2315–2330.

890 Elosegi, A., Dìez, J., Mutz, M., 2010. Effects of hydromorphological integrity on biodiversity
891 and functioning of river ecosystems. Hydrobiologia 657, 199–215.

892 Fitzpatrick, F. A., Knox, J. C., Schubauer-Berigan, J.P., 2009. Channel, floodplain, and wetland
893 responses to flood sand overbank sedimentation, 1846 2006, Halfway Creek Marsh , Upper
894 Mississippi Valley, Wisconsin: in James ,L. A. , Rathburn, S. L. , and Whittecar, G. R. ,eds.,
895 Management and Restoration of Fluvial Systems with Broad Historical Changes and Human
896 Impacts, Geological Society of America Special Paper 451, 23–42

897 Fruget J.F., 1992. Ecology of the Lower Rhône following 200 years of human influence: a
898 review. Regulated Rivers 7, 233–246

899 García-Ruiz, J.M., Lasanta, T., Ruiz-Flano, P., Ortigosa, L., White, S., González, C., Martí, C.,
900 1996. Land-use changes and sustainable development in mountain areas: a case study in the
901 Spanish Pyrenees. Landscape Ecology 11 (5), 267–277.

902 García-Ruiz, J.M., Lana-Renault, N., 2011. Hydrological and erosive consequences of
903 farmland abandonment in Europe, with special reference to the Mediterranean region - A
904 review. Agriculture, Ecosystems and Environment 140(3-4), 317–338.

905 Gautier, E., Corbonnois, J., Petit, F., Arnaud-Fassetta, G., Brunstein, D., Grivel, S.,
906 Houbrechts, G., Beck, T., 2009. Multidisciplinary approach for sediment dynamics study of
907 active floodplains. Géomorphologie: relief, processus, environnement 1, 65–78.

908 Girel, J., Vautier, F., Peiry, J. L., 2003. Biodiversity and land use history of the alpine riparian
909 landscapes (the example of the Isère river valley, France). Multifunctional landscapes 3, 167–
910 200.

911 Ghoshal, S, James, A., Singer, M. B., Aalto, R., 2010. Channel and floodplain change analysis
912 over a 100-year period: Lower Yuba River, California. Remote Sens 2, 1797–1825.

913 Gregory, K.J., 2006. The Human Role in Changing River Channels. Geomorphology 79(3),
914 172–191.

915 Guerrin, J., 2015. A floodplain restoration project on the River Rhône (France): analysing
916 challenges to its implementation. Regional Environmental Change 15 (3), 559–568.

Guertault, L., 2015. Évaluation des processus hydro-sédimentaires d'une retenue de forme allongée: application à la retenue de Génissiat sur le Haut-Rhône. Mécanique des fluides. Université Claude Bernard - Lyon I. Français.

Habersack, H., Piégay, H., 2007. Challenges in river restoration in the Alps and their surrounding areas. In: Habersack, H., Piégay, H. Rinaldi, M. *Gravel bed rivers 6: from process understanding to river restoration*. Elsevier Science, pp.703–737.

Harrison, L.R., Dunne, T., Fisher, G.B., 2015. Hydraulic and geomorphic processes in an overbank flood along a meandering, gravel-bed river: implications for chute formation. Earth Surface Processes and Landforms 40, 1239–1253.

Hobo, N., Makaske, B., Wallinga, J., Middelkoop, H., 2014. Reconstruction of eroded and deposited sediment volumes of the embanked River Waal, the Netherlands, for the period AD 1631–present. Earth Surface Processes Landforms 39, 1301–1318.

Hohensinner, S., Habersack, H., Jungwirth, M. and Zauner, G., 2004. Reconstruction of the characteristics of a natural alluvial river-floodplain system and hydro morphological changes following human modifications: the Danube River (1812 –1991). River Research and Applications 20, 25 – 41.

Hooke, J.M., 1995. River channel adjustment to meander cutoffs on the river Bollin and river Dane, northwest England. Geomorphology 14, 235–253.

Hoyle, J., Brooks, A., Brierley, G., Fryirs, K., Lander, J., 2008. Spatial variability in the timing, nature and extent of channel response to typical human disturbance along the Upper Hunter River, New South Wales, Australia. Earth Surface Processes and Landforms 33, 868–889. DOI:10.1002/esp.1580.

Hughes, M.L., McDowell, P.F., Marcus, W.A., 2006. Accuracy assessment of georectified aerial photographs: Implications for measuring lateral channel movement in a GIS. Geomorphology 74, 1–16.

942 Hupp, C.R. and Bazemore, D. E., 1993. Spatial and temporal aspects of sediment deposition
943 in West Tennessee forested wetlands. Journal of Hydrology 141, 179–196

944 IGN-Geoportail: https://www.geoportail.gouv.fr/

945 Jansson, R., Nilsson, C. and Renofalt, B., 2000. Fragmentation of Riparian Floras in Rivers
946 with Multiple Dams. Ecology 81, 899–903.

947 Jenkins, K. M., Boulton. A. J., 2003. Connectivity in a dryland river: short-term aquatic
948 microinvertebrate recruitment following floodplain inundation. Ecology 84, 2708–2723.

949 Junk, W. J., Bayley, P. B., Sparks. R. E., 1989. The flood pulse concept in river-floodplain
950 systems. In D.P. Dodge [ed.] Proceedings of the International Large River Symposium. Can.
951 Spec. Publ. Fish. Aquat. Sci. 106, 110–127.

952 Karaouzas, I., Lambropoulou, D.A., Skoulikidis, N.T., Albanis, T.A., 2011. Levels, sources and
953 spatiotemporal variation of nutrients and micropollutants in small streams of a Mediterranean
954 River basin. J Environ Monit. 13(11), 3064–3074.

955 Kondolf, M. G., et al., 2006. Process-based ecological river restoration: Visualizing three-
956 dimensional connectivity and dynamic vectors to recover lost linkages. Ecology and Society 11,
957 5.

958 Kondolf, M. G., Piégay, H. and Landon, N., 2007. Changes in the riparian zone of the lower
959 Eygues river, France, since 1830. Landscape Ecology 22, 367–384.

960 Kondolf, M. G., 1997. Hungry Water: Effects of Dams and Gravel Mining on River Channels
961 Environ Manage 21(4), 533–51.

962 Knox, J.C., 2006. Floodplain sedimentation in the Upper Mississippi Valley: Natural versus
963 human accelerated. Geomorphology 79(3–4), 286–310.

964 Krüger,F., Schwartz, R., Kunert, M., Friese, K., 2006. Methods to calculate sedimentation
965 rates of floodplain soils in the middle region of the Elbe River. Acta hydrochim. hydrobiol.
966 34, 175–87.

967 Le Coz, J., 2007. Fonctionnement hydro-sédimentaire des bras morts de rivière alluviale.
968 Thèse de doctorat. Ecully, Ecole centrale de Lyon. 308p.

969 Lespez, L., Garnier, E., Cador, J. M., Rocard, D., 2005. *Les aménagements hydrauliques et la*
970 *dynamique des paysages des petits cours d'eau depuis le XVIIIe siècle dans le nord-ouest de la*
971 *France: l'exemple du bassin versant de la Seulles (Calvados) [archive]*. Aestuaria, 7, 89–109.

972 Lewin, J., Bradley, S. B., Macklin, M. G., 1983. Historical valley alluviation in mid-Wales.
973 Geological Journal 19, 331–350.

974 Liébault, F. and Piégay, H., 2002. Causes of 20th century channel narrowing in mountain and
975 Piedmont Rivers of Southeastern France Earth Surface Processes and Landforms 27(4), 425–
976 444.

977 Magilligan, F.J., Graber, B.E., Nislow, K.H., Chipman, J.W., Sneddon, C.S. and Fox, C.A., 2016.
978 River restoration by dam removal: Enhancing connectivity at watershed scales. Elem Sci Anth,
979 4, p.000108.

980 Margui, E., Hidalgo, M., Queralt, I., Van Meel, K., Fontas, C., 2012. Analytical capa-bilities of
981 laboratory, benchtop and handheld X-ray fluorescence systems for detection of metals in
982 aqueous samples pre-concentrated with solid-phase extraction disks. Spectrochim. Acta Part B
983 At. Spectrosc. 67, 17–23.

984 Matys Grygar, T., Elznicová, J., Tůmová, Š., Faměra, M., Balogh, M., Kiss, T., 2016. Floodplain
985 architecture of an actively meandering river (the Ploučnice River, the Czech Republic) as
986 revealed by the distribution of pollution and electrical resistivity tomography. Geomorphology
987 254, 41–56.

988 Marteau, T., 1993. Bilan des extractions de granulats en lits mineurs. Etude BRGM R37872.
989 Ministère de l'Industrie, des Postes et Télécommunications et du Commerce extérieur. 14 pp.

990 Melquiades, F.L., Appoloni, C.R., 2004. Application of XRF and field portable XRF for
991 environmental analysis. Journal of Radioanalytical and Nuclear Chemistry 62 (2), 533–541.

992 Merritt, D.M. and Cooper D.J., 2000. Riparian vegetation and channel change in response to
993 river regulation: a comparative study of regulated and unregulated streams in the Green River
994 basin, USA. Regulated Rivers: Research and Management 16, 543–564.

995 Meybeck, M., Lestel, L., Bonte, P., Moilleron, R., Colin, J. L., Rousselot, O., Herve, D., De
996 Ponteves, C., Grosbois, C., Thevenot, D. R., 2007. Historical perspective of heavy metals
997 contamination (Cd, Cr, Cu, Hg, Pb, Zn) in the Seine River basin (France) following a DPSIR
998 approach (1950-2005). Sci. Total. Environ. 375 (1-3), 204–231.

999 Middelkoop, F.I., 2000. Heavy-metal pollution of the river Rhine and Meuse floodplains in
1000 The Netherlands. Netherlands Journal of Geosciences 79, 411–428.

1001 Nanson, G.C., and Beach, H.F., 1977. Forest succession and sedimentation on a meandering-
1002 river floodplain, northeast British Columbia, Canada. J. Biogeogr. 4, 229–251

1003 Nilsson, C. and Jansson, R., 1995. Floristic differences between riparian corridors of
1004 regulated and free-flowing boreal rivers. Regulated Rivers: Research and Management 11, 55–
1005 66.

1006 Nilsson C. and Berggren K., 2000. Alterations of riparian ecosystems resulting from river
1007 regulation. BioScience 50, 783–792.

1008 Nilsson C., Reidy C.A., Dynesius M., Revenga C., 2005. Fragmentation and flow regulation of
1009 the world's large river systems. Science 308, 405–408.

1010 Nilsson, C., Jansson, R. and Zinko, U., 1997. Long-term responses of river-margin vegetation
1011 to water-level regulation, Science 276, 798–800.

1012 Olivier, J.M., Carre, G., Lamouroux, N., Dole-Olivier, M.J., Malard, F., Bravard, J.P., et al.,
1013 2009. The Rhône River basin. In eds. Tockner, K. Uehlinger, U. Robinson, C. T. Rivers of Europe
1014 (Amsterdam: Academic Press), 247–295.

1015 Ollero, A., 2010. Channel changes and floodplain management in the meandering middle
1016 Ebro River, Spain. Geomorphology 117, 247–260.

1017 Seignemartin, G., Tena, A., Räpple, B., Arnaud, F., Barra, A., Berger, J.F., Faure, O., Launay,
1018 M., Le Coz, J., Roux, G., Massor, H., Winiarski, T., Piégay, H., 2018. Sédimentation et
1019 morphologie du lit majeur. Stocks sédimentaires des marges actives – Méthodologie générale
1020 et application sur Péage-de-Roussillon. Observatoire des Sédiments du Rhone, Action II.2 et
1021 Action II.4. 76 pp.

1022 Page, K.J., Nanson, G.C., Frazier P.S., 2003. Floodplain formation and sediment stratigraphy
1023 resulting from oblique accretion on the Murrumbidgee River, Australia. J. Sed. Res. 73, 5–14

1024 Parrot, E., 2015. Analyse spatio-temporelle de la morphologie du chenal du Rhône du Léman
1025 à la Méditerranée. Lyon 3 University. Ph.D. Thesis.

1026 Peiry, J.L., 1997. Recherche en géomorphologie fluviale dans les hydrosystèmes fluviaux des
1027 Alpes de Nord. H.D.R., Université Joseph Fourier, Institut de Géographie Alpine, Grenoble.

1028 Petts, G.E., 1984. Impounded Rivers: Perspectives for Ecological Management. John Wiley
1029 and Sons Ltd, London.

1030 Petts, G.E., 1989. Historical change of large alluvial rivers. Western Europe, Wiley, London

1031 Piégay, H., Walling, D.E., Landon, N., He, Q., Liébault, F., Petiot. R., 2004. Contemporary
1032 changes in sediment yield in an alpine mountain basin due to afforestation (the upper Drôme
1033 in France). Catena 55 (2), 183–212.

1034 Piégay, H., Alber, A., Slater, L., Bourdin, L., 2009. Census and typology of braided rivers in
1035 the French Alps. Aquatic Sciences 71, 371–388.

1036 Piégay, H., Hupp, C.R., Citterio, A., Dufour, S., Moulin, B., Walling, D.E., 2008. Spatial and
1037 temporal variability in sedimentation rates associated with cut off channel infill deposits: Ain
1038 River, France. Water Resour. Res. 44, Article W05420.

1039 Piégay, H., Aelbrecht, D., Béal, D., Alonso, C., Armburster, J., Arnaud, F., Barillier, A., Béraud,
1040 C., Billard, C., Bouchard. J. P., 2010. Restauration morpho-dynamique et redynamisation de la

1041 section court-circuitée du Rhin en aval du barrage de Kembs (projet INTERREG/EDF). In
1042 *Congrès SHF:" Environnement et Hydro-électricité"*, 8–p.

1043 Poinsart, D., 1992. Effets des aménagements fluviaux sur les débits liquides et solides :
1044 l'exemple du Rhône dans les plaines de Miribel-Jonage et de Donzère-Mondragon. Thèse :
1045 Géographie et Aménagement : Lyon 3

1046 Poirier, N., 2006. Des plans terriers au cadastre ancien: Mesurer l'évolution de l'occupation
1047 du sol grâce au SIG [archive]. Le médiéviste et l'ordinateur, 44. Institut de Recherche et
1048 d'Histoire des Textes, CNRS, Paris. http://lemo.irht.cnrs.fr/44/plans-terriers.htm.

1049 Phillips, J. D., 2003. Toledo Bend Reservoir and geomorphic response in the lower Sabine
1050 River. River Research and Applications 19, 137–159.

1051 Provansal, M., Raccasi, G., Monaco, M., Robresco, S., Dufour, S., 2012. La réhabilitation des
1052 marges fluviales, quel intérêt, quelles contraintes? Le cas des annexes fluviales du Rhône aval.
1053 Méditerranée 118, 85–94.

1054 Räpple, B., 2018. Sedimentation patterns and riparian vegetation characteristics in novel
1055 ecosystems on the Rhône River, France. A comparative approach to identify drivers and
1056 evaluate ecological potentials. Lyon University (Ecole Normale Supérieure de Lyon). Ph.D.
1057 Thesis.

1058 Riquier, J., 2015. Réponses hydrosédimentaires de chenaux latéraux restaurés du Rhône
1059 français. Structures spatiales et dynamiques temporelles des patrons et des processus,
1060 pérennité et recommandations opérationnelles, Lyon 2 University. Ph.D. Thesis.

1061 Roditis, J.C., Pont, D., 1993. Dynamiques fluviales et milieux de sédimentation du Rhône a
1062 l'amont immédiat de son delta. Méditerranée 3(4), 5–18.

1063

1064 Roni, P., Hall, J. E., Drenner, S. M., Arterburn, D., 2019. Monitoring the effectiveness of
1065 floodplain habitat restoration: A review of methods and recommendations for future
1066 monitoring. WIREs Water 6, e1355. https://doi.org/10.1002/wat2.1355

1067 Rouillon, M., Taylor, M. P., 2016. Can field portable X-ray fluorescence (pXRF) produce high
1068 quality data for application in environmental contamination research?. Environ Pollut. 214,
1069 255–264.

1070 Schiemer, F., Baumgartner, C. and Tockner, C., 1999. Restoration of floodplain rivers: the
1071 Danube Restoration project. Reg. Rivers: Res. Mgmt. 15, 231–244.

1072 Smith, N. D., Morozova, G. S., Pérez-Arlucea, M. Gibling, M. R., 2016. Dam-induced and
1073 natural channel changes in the Saskatchewan River below the E.B. Campbell Dam, Canada .
1074 Geomorphology 269, 186 –202.

1075 Schwartz, R. and Kozerski, H., 2003. Entry and deposits of suspended particulate matter in
1076 groyne fields of the middle Elbe and its ecological relevance, Acta Hydrochimica et
1077 Hydrobiologica 31(4-5), 391 – 399.

1078 Scorpio, V., Rosskopf, C.M., 2016. Channel adjustments in a Mediterranean river over the
1079 last 150 years in the context of anthropic and natural controls. Geomorphology 275, 90–104.

1080 Shields, F. D., Jr., Knight, S. S., Lizotte R. Jr., Wren, D. G., 2011. Connectivity and variability:
1081 Metrics for riverine floodplain backwater rehabilitation, in Stream Restoration in Dynamic
1082 Fluvial Systems: Scientific Approaches, Analyses, and Tools, Geophys. Monogr. Ser., vol. 194,
1083 edited by A. Simon et al., pp. 233–246, AGU, Washington, D. C.

1084 Simons, J., Barker, C., Schropp, M., Jans, L., Kok, F., Grift R., 2001. Man-made secondary
1085 channels along the river Rhine (the Netherlands); results of post-project monitoring. River
1086 Research and Applications17 (4–5), 473–491.

1087 Singh, H., Singh, D., Singh S. K., Shukla D. N., 2017. Assessment of river water quality and
1088 ecological diversity through multivariate statistical techniques, and earth observation dataset

1089 of rivers Ghaghara and Gandak, India. International Journal of River Basin Management 15 (3),
1090 347–360.

1091 Surian, N., 1999. Channel changes due to river regulation: the case of the Piave River, Italy.
1092 Earth Surface Processes and Landforms 24, 1135 –1151.

1093 Surian, N., Rinaldi, M., 2003. Morphological response to river engineering and management
1094 in alluvial channels in Italy. Geomorphology 50, 307 –326.

1095 Terrado, M., Barceló, D., Tauler, R., 2006. Identification and distribution of contamination
1096 sources in the Ebro river basin by chemometrics modelling coupled to geographical
1097 information systems. Talanta 70, 691–704.

1098 Thorel M., Piégay H., Barthelemy C., B Räpple, Gruel C-R., Marmonier P., Winiarski T., Bedell
1099 J-P., Arnaud F., Roux G., Stella J. C., Seignemartin G., Tena A., Wawrzyniak V., Roux-Michollet
1100 D., Oursel B., Fayolle S., Bertrand C., Franquet E., 2018. Socio-environmental stakes associated
1101 with process-based restoration strategies in large rivers: should we remove novel ecosystems
1102 along the Rhône? Regional Environmental Change 18(7), 2019–2031.

1103 Tockner, K. and Stanford J.A., 2002. Riverine flood plains: present state and future trends.
1104 Environmental Conservation 29, 308–330.

1105 Tockner, K., Schiemer, F. and Ward, J., 1998. Conservation by restoration: the management
1106 concept for a river-floodplain system on the Danube River in Austria. Aquatic Conservation:
1107 Marine Freshwater Ecosystems 8, 71–86.

1108 Tracy-Smith, E., Galat, D.L., Jacobson, R.B., 2012. Effects of flow dynamics on the aquatic-
1109 terrestrial transition zone (ATTZ) of the lower Missouri River sand bars with implications for
1110 selected biota. River Research and Applications 28 (7), 793–813.

1111 Vauclin, S., Mourier, B., Seignemartin, G., Tena, A., Develle, A.L., Piégay, H., Berger, J.F.,
1112 Winiarski, T. (submitted) Characterizing the infrastructure-induced legacy sediments by a
1113 combined geophysical and coring approach

1114 Vázquez-Tarrío, D., Tal, M., Camenen, B., Piégay, H., 2018. Effects of continuous
1115 embankments and successive run-of-the-river dams on bedload transport capacities along the
1116 Rhône River, France. Science of the Total Environment 658, 1375–1389.

1117 Vericat, D., Brasington, J., Wheaton, J., Cowie, M., 2009. Accuracy assessment of aerial
1118 photographs acquired using lighter-than-air blimps: low-cost tools for mapping river corridors.
1119 River Research and Applications 25, 985–1000.

1120 Walling, D. E., He, Q., 1997. Models for converting 137 Cs measurements to estimates of soil
1121 redistribution rates on cultivated and uncultivated soils (including software for model
1122 implementation). Report to IAEA. University of Exeter, UK.

1123 Ward JV, Tockner K, Schiemer F., 1999. Biodiversity of floodplain river ecosystems: Ecotones
1124 and connectivity. Regulated Rivers: Research and Management 15, 125–139.

1125 Ward, J. V., Stanford, J. A., 1995. Ecological connectivity in alluvial river ecosystems and its
1126 disruption by flow regulation. Regul. Rivers: Res. Manage. 11, 105–119.

1127 Ward, J.V., 1998. Riverine landscapes: biodiversity patterns, disturbance regimes, and
1128 aquatic conservation. Biological Conservation 83 (3), 269–278.

1129 White, W.A., Morton, R.A., Holmes, C.W., 2002. A comparison of factors controlling
1130 sedimentation rates and wetland loss in fluvial-deltaic systems, Texas Gulf coast.
1131 Geomorphology 44, 47–66

1132 Williams, G.P., 1978. Bank-full discharge of rivers. Water Resources Research 14(6), 1141–
1133 1154.

1134 Wohl, E., 2004. Limits of downstream hydraulic geometry. Geology 32 (10), 897–900. doi:
1135 https://doi.org/10.1130/G20738.1

1136 Wohl, E., Angermeier, P.L., Bledsoe, B., Kondolf, G.M., MacDonnell, L., Merritt, D.M.,
1137 Palmer, M.A., Poff, N.L., Tarboton, D., 2005. River restoration. Water Resources Research 41,
1138 W10301.

1139 Woitke, P., Wellmitz, J., Helm, D., Kube, P., Lepom, P. and Litheraty, P., 2003. Analysis and
1140 assessment of heavy metal pollution in suspended solids and sediments of the river Danube.
1141 Chemosphere 51, 633–642.

1142 Wyżga, B., 2001. Impact of the channelization-induced incision of the Skawa and Wisłoka
1143 Rivers, southern Poland, on the conditions of overbank deposition. Regul. Rivers: Res. Mgmt.
1144 17, 85–100.

1145 Young, K.E., Evans, C.A., Hodges, K.V., Bleacher, J.E., Graff, T.G., 2016. A review of the
1146 handheld X-ray fluorescence spectrometer as a tool for field geologic investigations on Earth
1147 and in planetary surface exploration. Applied Geochemistry 72, 77–87. doi:10.1016
1148 /j.apgeochem.2016.07.003

1149 Yu, G.-A., Disse, M., Huang, H. Q., Yu, Y., Li, Z., 2016. River network evolution and fluvial
1150 process responses to human activity in a hyper-arid environment – Case of the Tarim River in
1151 Northwest China. Catena 147, 96–109

1152
1153
1154

Table 1. Main drivers of change and channel responses in the literature

Reference	River	Country	Study reaches (km or km^2)	Main Drivers of change	Channel responses	Methods
Allred and Schmidt (1999)	Green River	EEUU	25 km	Flow regulation/Climate change/Vegetation colonisation	Channel narrowing/ Bed degradation	Planform changes (Aerial imagery)/Bed elevation changes (cross sections), dendrochronology
Arnaud et al. (2015)	Upper Rhine	France	50 km	Flow regulation/Bank protection	Channel narrowing/Bed elevation changes (erosion and aggradation)/Floodplain sedimentation	Planform changes (Aerial imagery)/Bed elevation changes
Cadol et al. (2011)	Canyon del muerto Canyon de Chely	EEUU	50 km	Flow regulation/ Land use changes	Planform change/Channel narrowing/Vegetation encroachment	Planform changes (Aerial imagery, historical maps)
David et al. (2016)	Middle Garonne	France	90 km	Flow regulation/Bank protection/Gravel Mining	Channel narrowing/ Bed degradation/Floodplain stabilisation	Planform changes (Aerial imagery, historical maps)
Downs et al. (2013)	Lower Santa Clara	EEUU	55 km	Numerous natural and human drivers of change (Ranching, Irrigation, Regulation, Wildfires, earthquakes, etc.	Changes in channel width/Bed degradation	Planform changes (Aerial imagery)/Bed elevation changes (cross sections), GSD
Fitzpatrick and Knox (2000)	North Fish Creek	EEUU	121 km^2	Deforestation/Land use changes/Floods	Channel widening/Bed elevation changes (erosion and aggradation)/Floodplain sedimentation, Changes in sediment delivery	Planform changes (Aerial imagery, historical maps)/Bed elevation changes(cross sections)/Hydraulic and sediment transport modelling/Core analysis (Radiocarbon, Caesium, Metal tracers)
Ghoshal et al. (2010)	Lower Yuba	EEUU	12 km	Flow regulation/Gold mining	Channel aggradation	Planform changes (Aerial imagery, historical maps)/Bed elevation changes (cross sections)
Hohensinner et al. (2004)	Danube	Austria	10.25 km	Flow regulation/Bank protection	Planform change/Channel narrowing/ Floodplain sedimentation	Planform changes (Aerial imagery, historical maps)
Hoyle et al. (2008)	Hunter	Australia	12.5 km	Flow regulation/Human settlement	Planform change/Channel widening	Planform changes (Lidar, Aerial imagery, historical maps)/Bed elevation changes (cross sections)
Knox (2006)	Mississippi and tributaries	EEUU	-	Land use changes/ Metal mining	Floodplain aggradation	Core analysis (Radiocarbon, Caesium, Metal tracers)
Kondolf et al. (2007)	Lower Eygues	France	19 km	Land use changes/ Gravel mining	Channel narrowing/Bed elevation changes (erosion and aggradation)/Vegetation encroachment	Planform changes (Aerial imagery)/Bed elevation changes (cross sections), GSD

Ollero (2010)	Middle Ebro	Spain	346 km	Flow regulation/ Bank protection/Land Use Changes	River stabilisation/Vegetation encroachment	Planform changes (Aerial imagery, historical maps)
Scorpio and Rosskopf (2016)	Fortore	Italy	110 km	Flow regulation/ Gravel mining	Channel narrowing/Bed elevation changes (erosion and aggradation)/Changes in channel width	Planform changes (Aerial imagery, historical maps)
Smith et al.(2016)	Saskatchewan	Canada	108 km	Flow regulation/ Land use changes	Changes in channel width/Bedload transport decrease/Bed coarsening	Vertical changes (cross sections)/Bedload transport, GSD
Surian (1999)	Piave	Italy	110 km	Flow regulation/Bank protection/Gravel mining	Planform change/Channel narrowing/ Bed degradation	Planform changes (Aerial imagery, historical maps)
Winterbottom (2000)	Tummel	UK	12.5 km	Flow regulation/Bank protection	Channel narrowing/Bed elevation changes (erosion and aggradation)/Vegetation encroachment	Planform changes (Aerial imagery)
Yu et al. (2016)	Tarim	China	900 km	Flow regulation/Bank protection/Human settlement/Deforestation	Changes in channel planform/Sediment transport decrease/Disconnection from tributaries	Planform changes (Aerial imagery, historical Maps)/Bed elevation changes (cross sections)

Table 2. The number of surface sediment samples for each section and sedimentation period.

Sector	Sedimentation period	Metal rod probes (n)	Surface sediment samples (n)
PBN	Before 1860	71	35
	1860-1905	80	43
	1905-1945	227	115
	1945-1954	45	33
	1954-1993	184	83
	1993-2008	9	7
	2008-2016	3	1
PDR	1810-1860	518	5
	1860-1905	199	39
	1905-1938	108	26
	1938-1949	40	9
	1949-1974	35	11
	1974-1986	135	49
	1986-2009	111	27
	2009-2016	6	0
DZM	1810-1860	49	37
	1860-1947	126	65
	1947-1955	77	54
	1955-1976	241	90
	1976-2007	46	18
	2007-2016	56	2

1171 **Table 3.** Trace element concentrations observed in surface sediment samples obtained from

1172 PBN, PDR and DZM floodplains.

		Ni (mg kg^{-1})	Cu (mg kg^{-1})	Zn (mg kg^{-1})	Pb (mg kg^{-1})
	Median	38.52	43.26	153.6	44.51
PBN	**Max**	155.7	528.96	1021.38	7527.18
(n=317)	**Min**	5.22	0.63	58.84	13.08
	SD	11.43	57.34	107.31	433.8
	Median	36.72	37.47	148.24	31.97
PDR	**Max**	53.84	170.33	298.53	65.45
(=166)	**Min**	25.59	19.81	77.69	7.53
	SD	5.09	12.88	38.21	12.35
	Median	42.28	33.86	127.79	35.91
DZM	**Max**	60.69	241.87	613.43	163.19
(=266)	**Min**	15.83	14.23	71.46	13.44
	SD	5.17	14.05	36.88	16.66

1173

1174

Figures Caption

Figure 1. A, Location of the Rhône Basin in France and location of the study areas in the Rhône Basin (Pierre-Bénite, PBN; Péage-de-Roussillon, PDR; and Donzère-Mondragon, DZM). The PDR is displayed to present information obtained and generated for each section: B, Active zone in different periods, C, Floodplain flooding frequency, and D, Locations of overbank sediment depths estimated by rod sampling.

Figure 2. Rhône channel planform evolution in the three studied reaches: A, PBN; B, PDR; and C, DZM. Colours indicate periods in which active channel areas were terrestrialised.

Figure 3. Example to illustrate the methodology followed for sediment rate determination.

Figure 4. Scatterplot showing the relation between ICP-MS and XRF concentrations for: A, Nickel; B, Copper; C, Zinc, and D, Lead.

Figure 5. A, Comparisons of the evolution of mean active channel widths of the Rhône River between 1810 and 2009 and B, Comparison of the evolution of the active channel area (%) of the Rhône River between 1810 and 2009 (because of a lack of data on PBN for 1810, the 100% value is based on data for 1860). Long dashed lines correspond to the Girardon phase, and short dashed lines correspond to channel bypassing for each of the sections.

Figure 6. Evolution of the mean number of flowing channels of the Rhône River per 100-m-long segment from 1810 to 2009. Long dashed lines correspond to the Girardon phase, and short dashed lines correspond to channel bypassing in each section. It should be noted that the size of DZM reach is much larger than PBN and PDR (28, 11.2 and 15.7 km, respectively).

Figure 7. A, Cumulative average active channel width and B, cumulative number of flowing channels per 100-m-long segment for the different periods for PBN, PDR and, DZM. It should be noted that the size of DZM reach is much larger than PBN and PDR (28, 11.2 and 15.7 km, respectively).

Figure 8. A, Relative thickness of the upper gravel layer relative to thalweg elevation (Dzubakova et al., 2015), B, Fine sediment thickness, and C, Fine sedimentation rates according to the period of floodplain terrestrialisation in PBN, PDR and DZM. Long dashed lines denote Girardon dike systems, and short dashed lines denote channel bypassing patterns of each of the sections. The variability is shown by 1st and 3rd quartiles (1st and 3rd Q in the legend).

Figure 9. Sedimentation rates of Girardon casiers and recently disconnected channels by period of floodplain terrestrialisation for A, PBN, B, PDR and C, DZM. The variability is shown by 1st and 3rd quartiles (1st and 3rd Q in the legend).

Figure 10. Comparison of metallic element concentrations contained in surface floodplain sediments by terrestrialisation period for PBN, PDR and DZM. Long dashed lines correspond to Girardon structures, and the short dashed lines denote channel bypassing in each of the sections. The variability is shown by 1st and 3rd quartiles (1st and 3rd Q in the legend).

Figure 11. Median present connection frequency by floodplain terrestrialisation period. Long dashed lines correspond to Girardon structures, and short dashed lines denote channel bypassing trends of each of the sections.

Figure 12. Scatterplot showing the link between median connection frequency and the median A, Floodplain elevation, B, Gravel thickness, C, Fine sediment thickness and, D, The sedimentation rate for each of the three studied reaches.

Figure 13. Scatterplot showing the link between median connection frequency and median concentrations of A, Nickel; B, Copper; C, Zinc, and D, Lead for each of the three studied reaches.

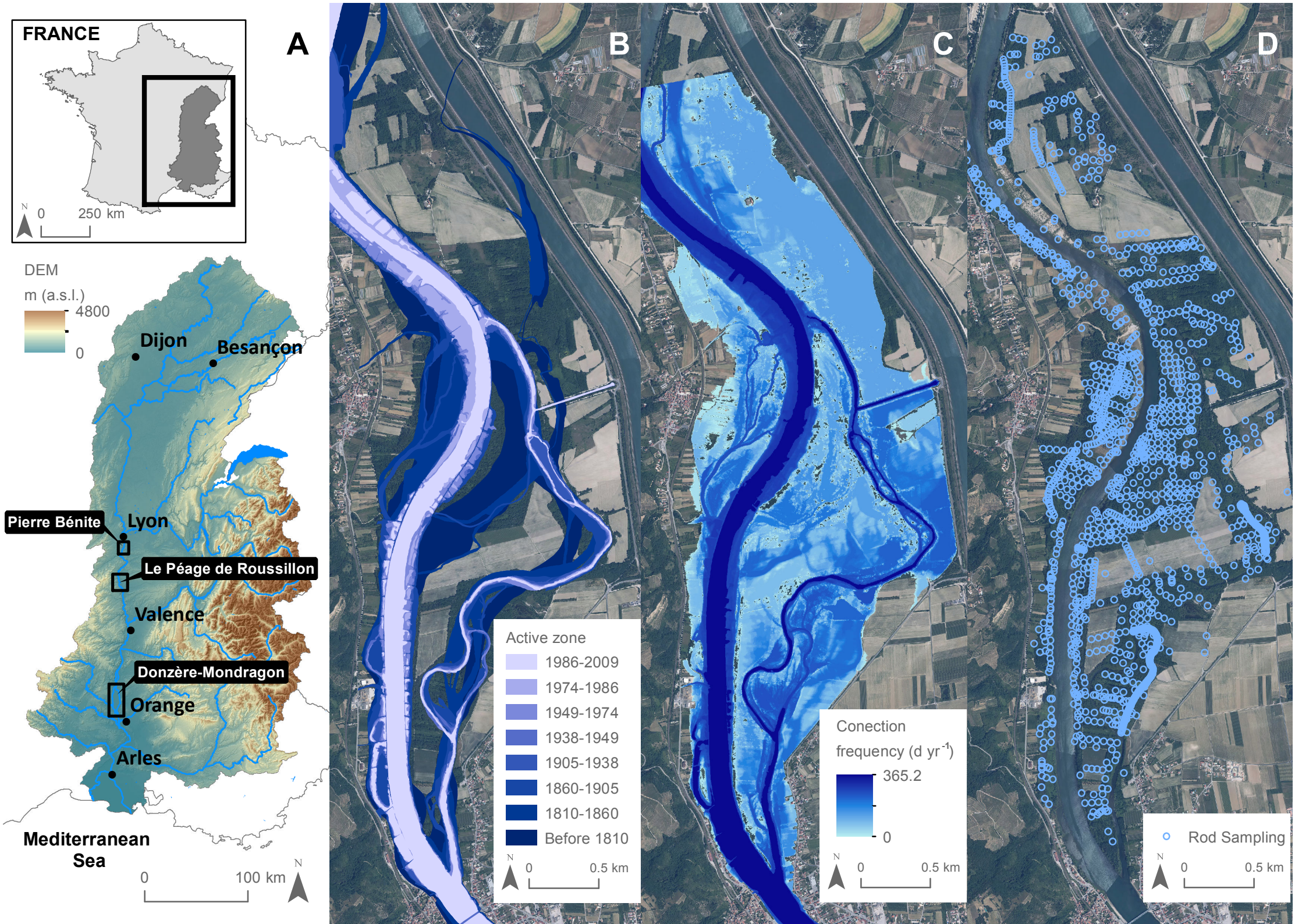
FRANCE
A
N
0
250 km
DEM
m (a.s.l.)
4800
0
Dijon
Besançon
Pierre Bénite
Lyon
Le Péage de Roussillon
Valence
Donzère-Mondragon
Orange
Arles
Mediterranean Sea
0
100 km
N
B
C
D
Active zone
1986-2009
1974-1986
1949-1974
1938-1949
1905-1938
1860-1905
1810-1860
Before 1810
N
0
0.5 km
Conection frequency (d yr-1)
365.2
0
N
0
0.5 km
Rod Sampling
N
0
0.5 km

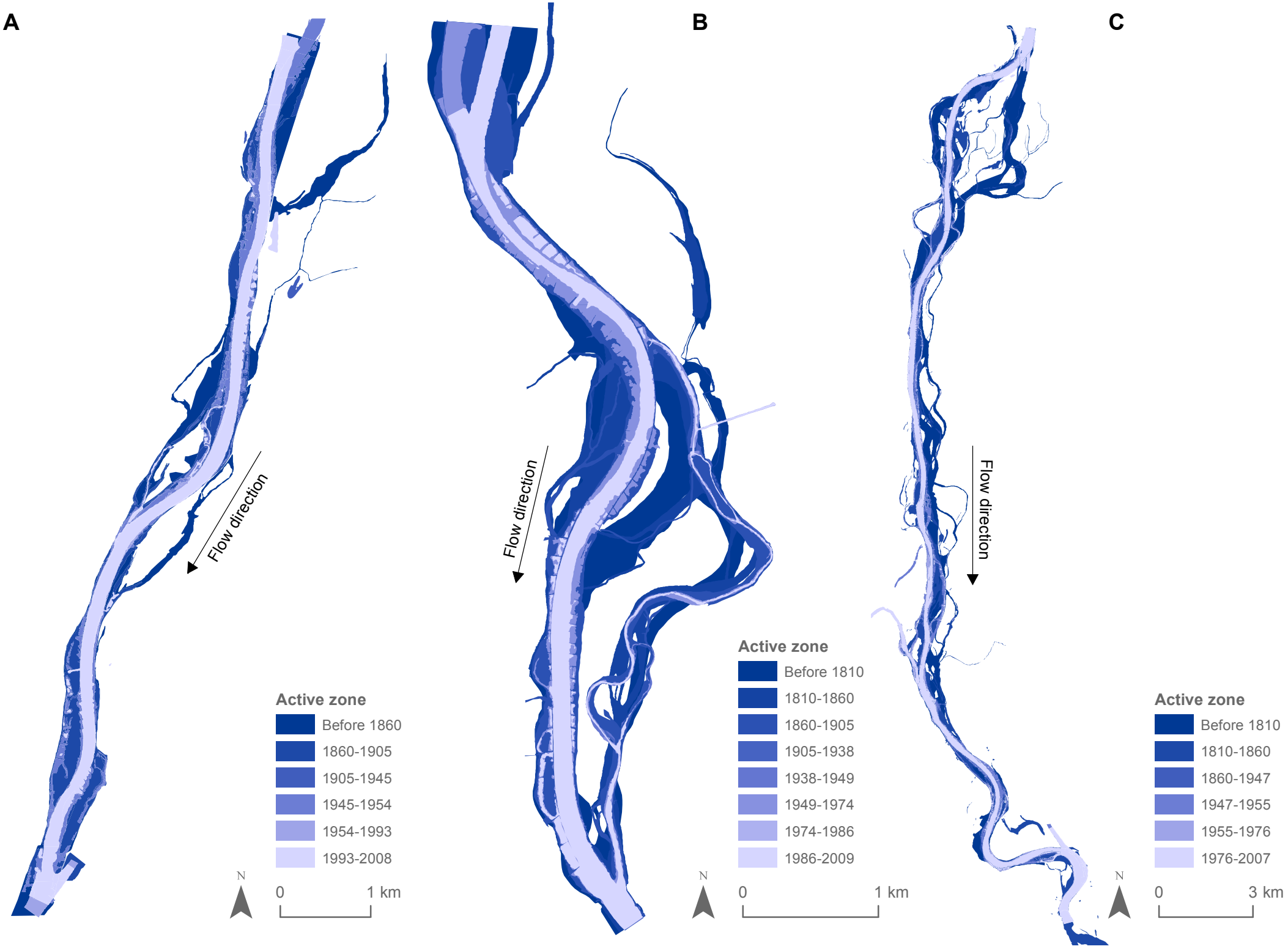
A
Flow direction
Active zone
Before 1860
1860-1905
1905-1945
1945-1954
1954-1993
1993-2008
N
0
1 km
B
Flow direction
Active zone
Before 1810
1810-1860
1860-1905
1905-1938
1938-1949
1949-1974
1974-1986
1986-2009
N
0
1 km
C
Flow direction
Active zone
Before 1810
1810-1860
1860-1947
1947-1955
1955-1976
1976-2007
N
0
3 km

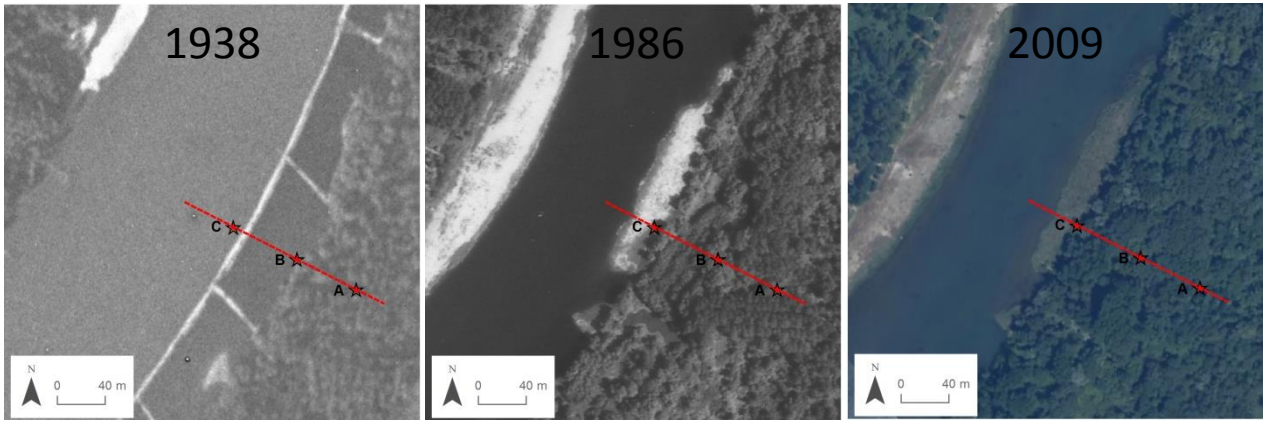
1938
1986
2009
C
B
A
N
0
40 m

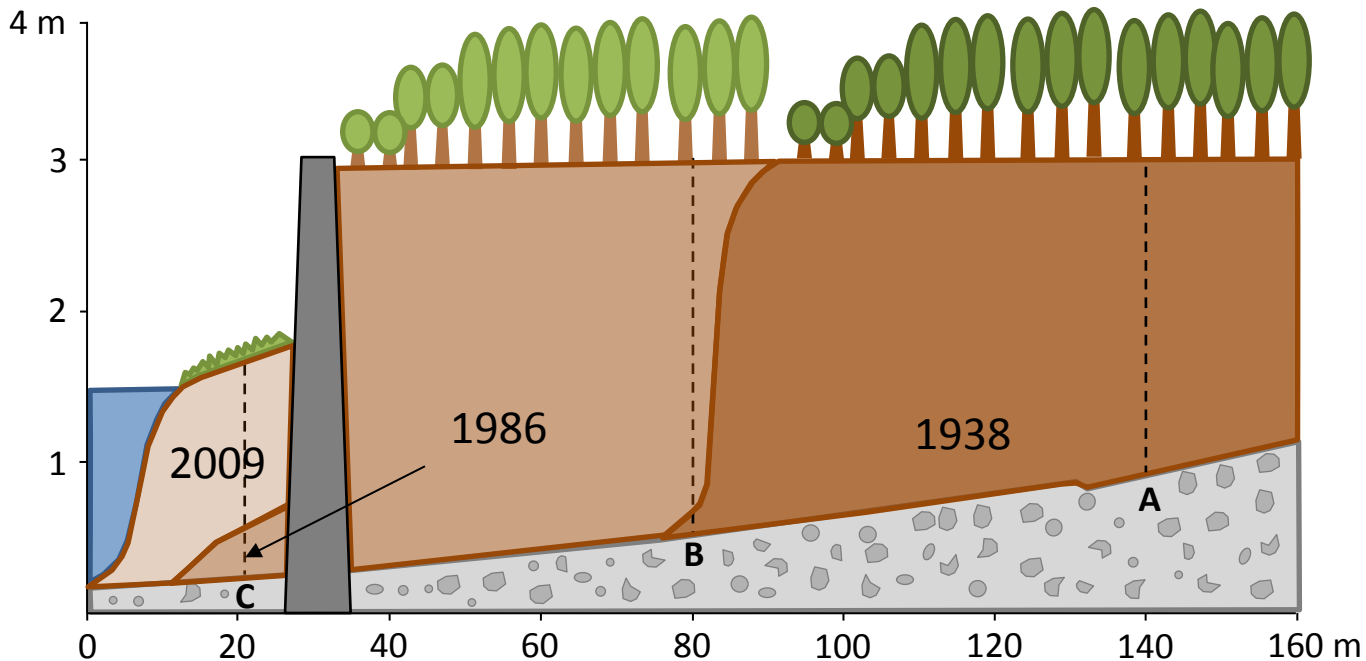
4 m
3
2
1
2009
1986
1938
A
B
C
0
20
40
60
80
100
120
140
160 m

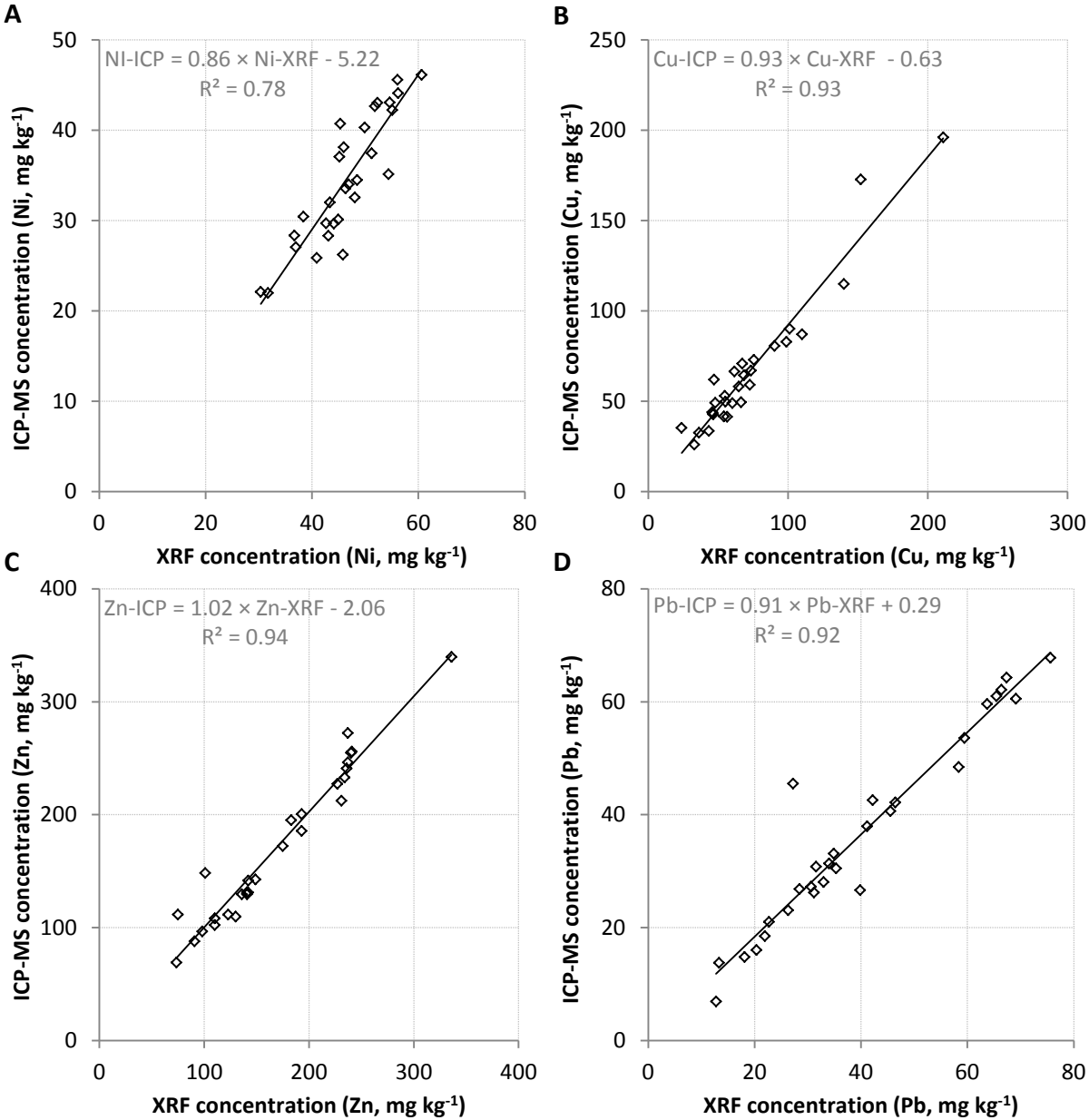
A
NI-ICP = 0.86 × Ni-XRF - 5.22
R² = 0.78
ICP-MS concentration (Ni, mg kg-1)
XRF concentration (Ni, mg kg-1)
B
Cu-ICP = 0.93 × Cu-XRF - 0.63
R² = 0.93
ICP-MS concentration (Cu, mg kg-1)
XRF concentration (Cu, mg kg-1)
C
Zn-ICP = 1.02 × Zn-XRF - 2.06
R² = 0.94
ICP-MS concentration (Zn, mg kg-1)
XRF concentration (Zn, mg kg-1)
D
Pb-ICP = 0.91 × Pb-XRF + 0.29
R² = 0.92
ICP-MS concentration (Pb, mg kg-1)
XRF concentration (Pb, mg kg-1)

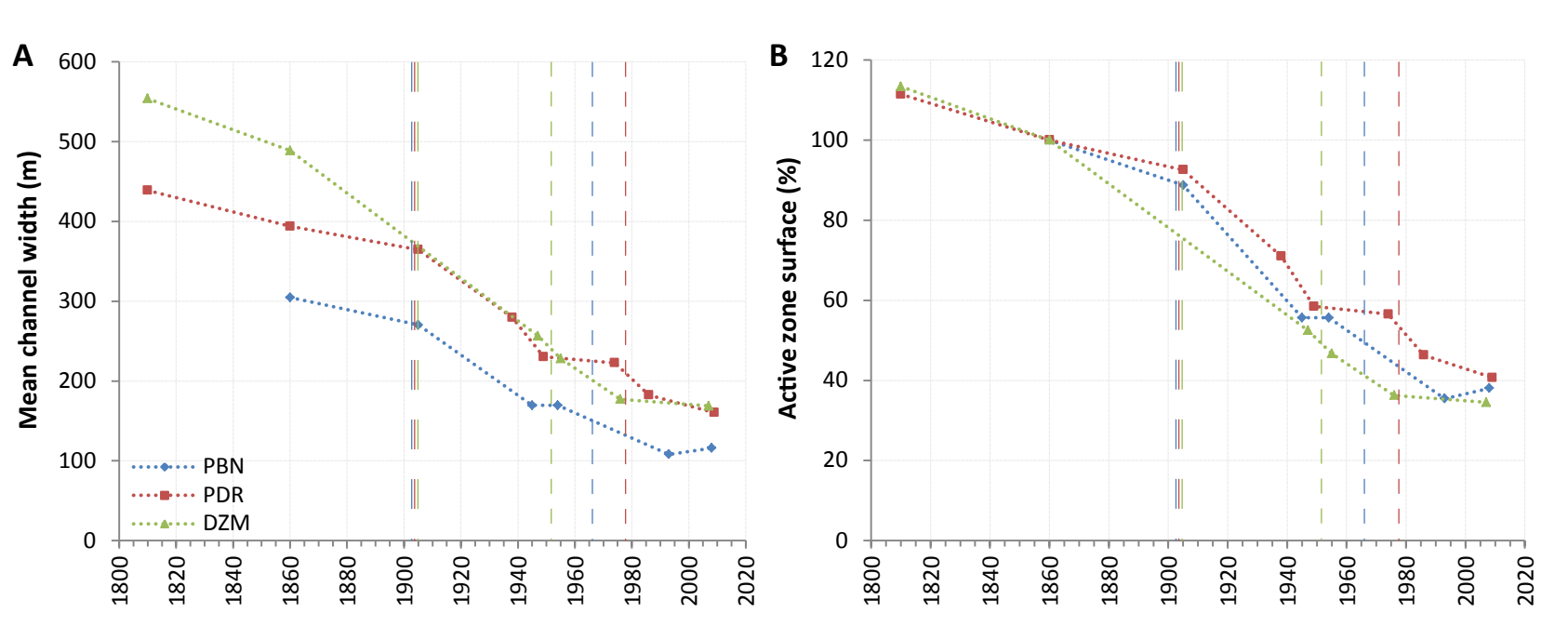
A
Mean channel width (m)
600
500
400
300
200
100
0
PBN
PDR
DZM
1800
1820
1840
1860
1880
1900
1920
1940
1960
1980
2000
2020
B
Active zone surface (%)
120
100
80
60
40
20
0
1800
1820
1840
1860
1880
1900
1920
1940
1960
1980
2000
2020

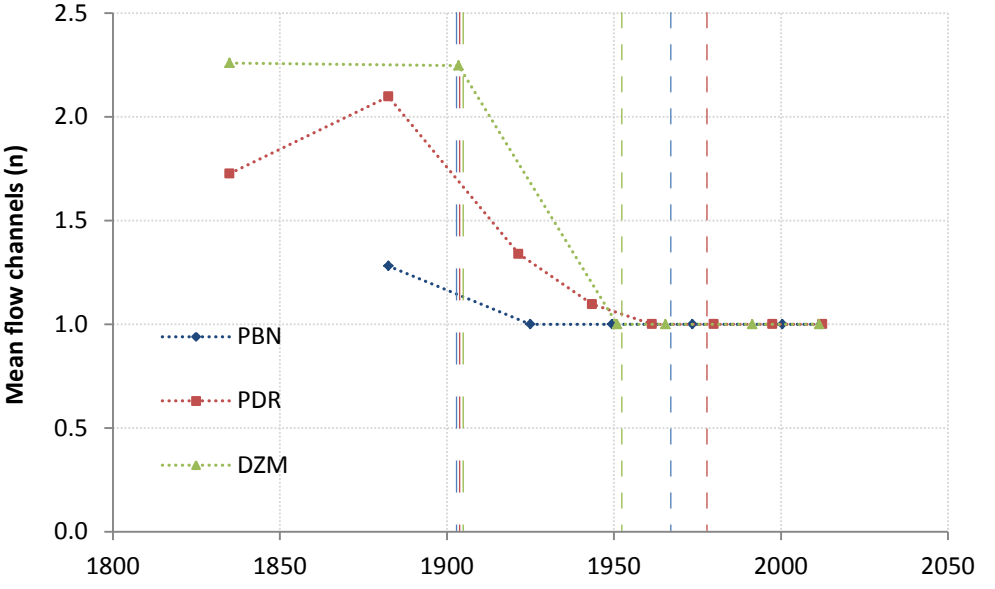
Mean flow channels (n)
2.5
2.0
1.5
1.0
0.5
0.0
1800
1850
1900
1950
2000
2050
PBN
PDR
DZM

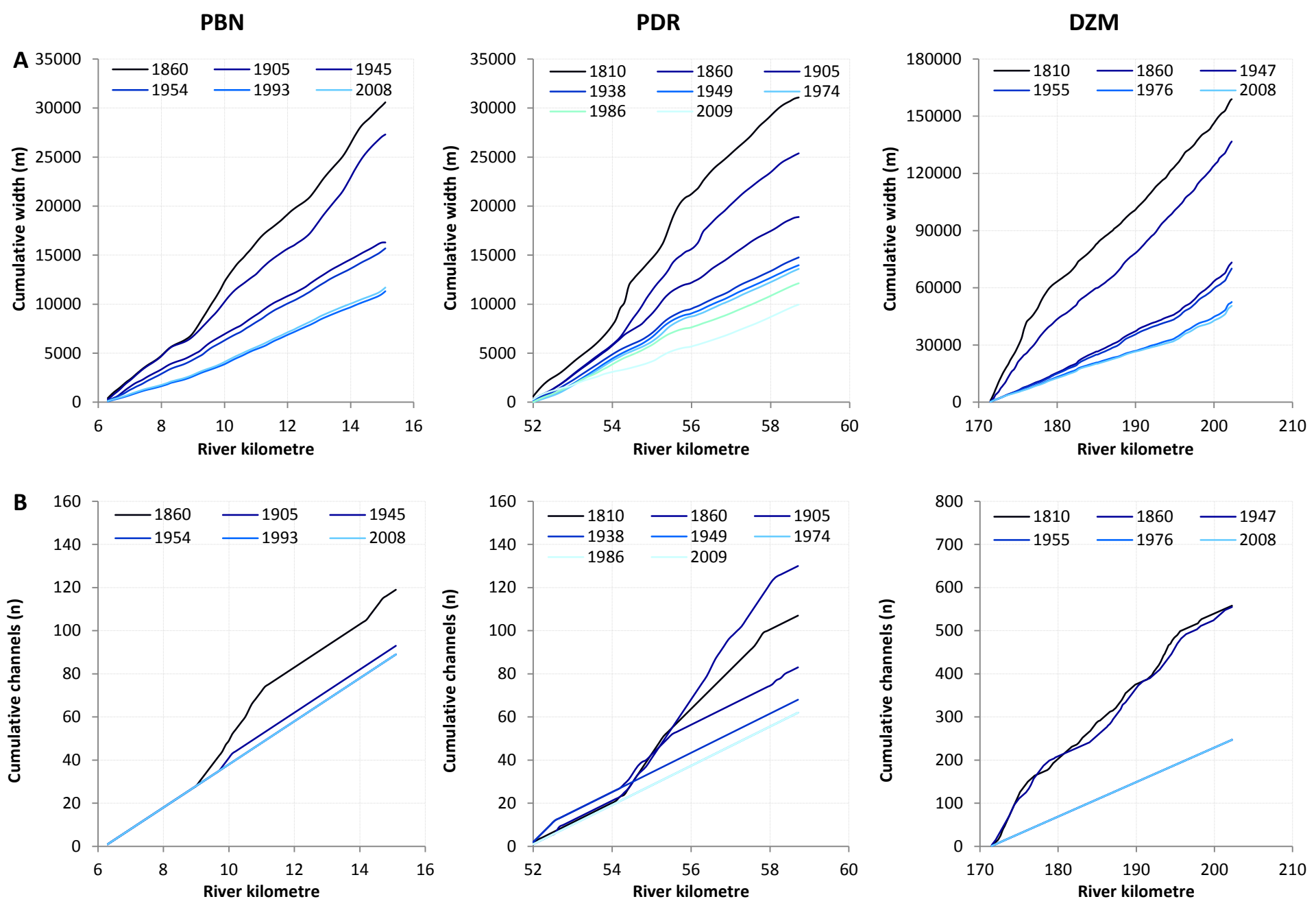
PBN
PDR
DZM
A
B
Cumulative width (m)
Cumulative channels (n)
River kilometre
1860
1905
1945
1954
1993
2008
1810
1938
1986
1949
1974
2009
1947
1955
1976

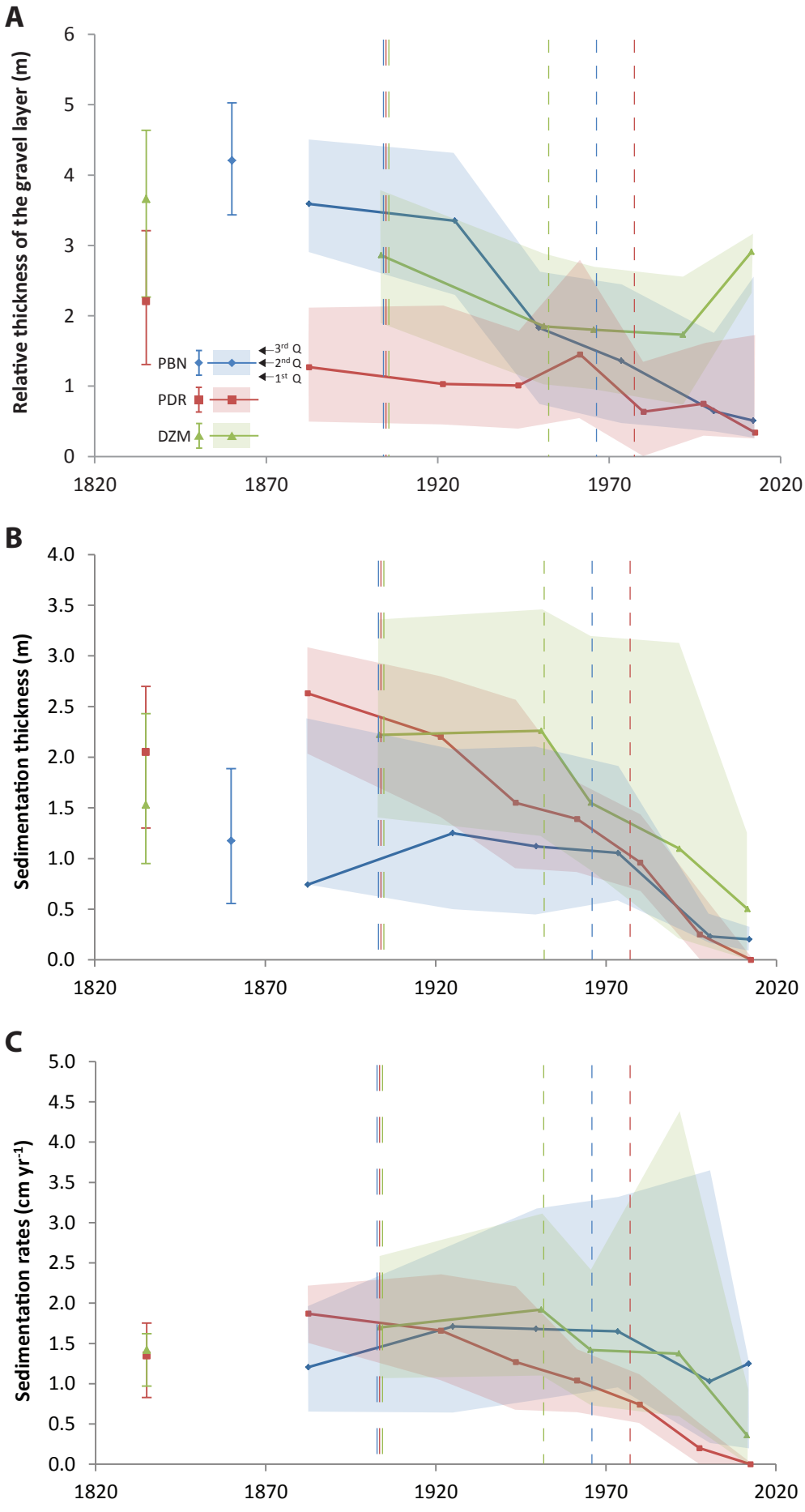
A
Relative thickness of the gravel layer (m)
0
1
2
3
4
5
6
1820
1870
1920
1970
2020
PBN
PDR
DZM
3rd Q
2nd Q
1st Q
B
Sedimentation thickness (m)
0.0
0.5
1.0
1.5
2.0
2.5
3.0
3.5
4.0
1820
1870
1920
1970
2020
C
Sedimentation rates (cm yr-1)
0.0
0.5
1.0
1.5
2.0
2.5
3.0
3.5
4.0
4.5
5.0
1820
1870
1920
1970
2020

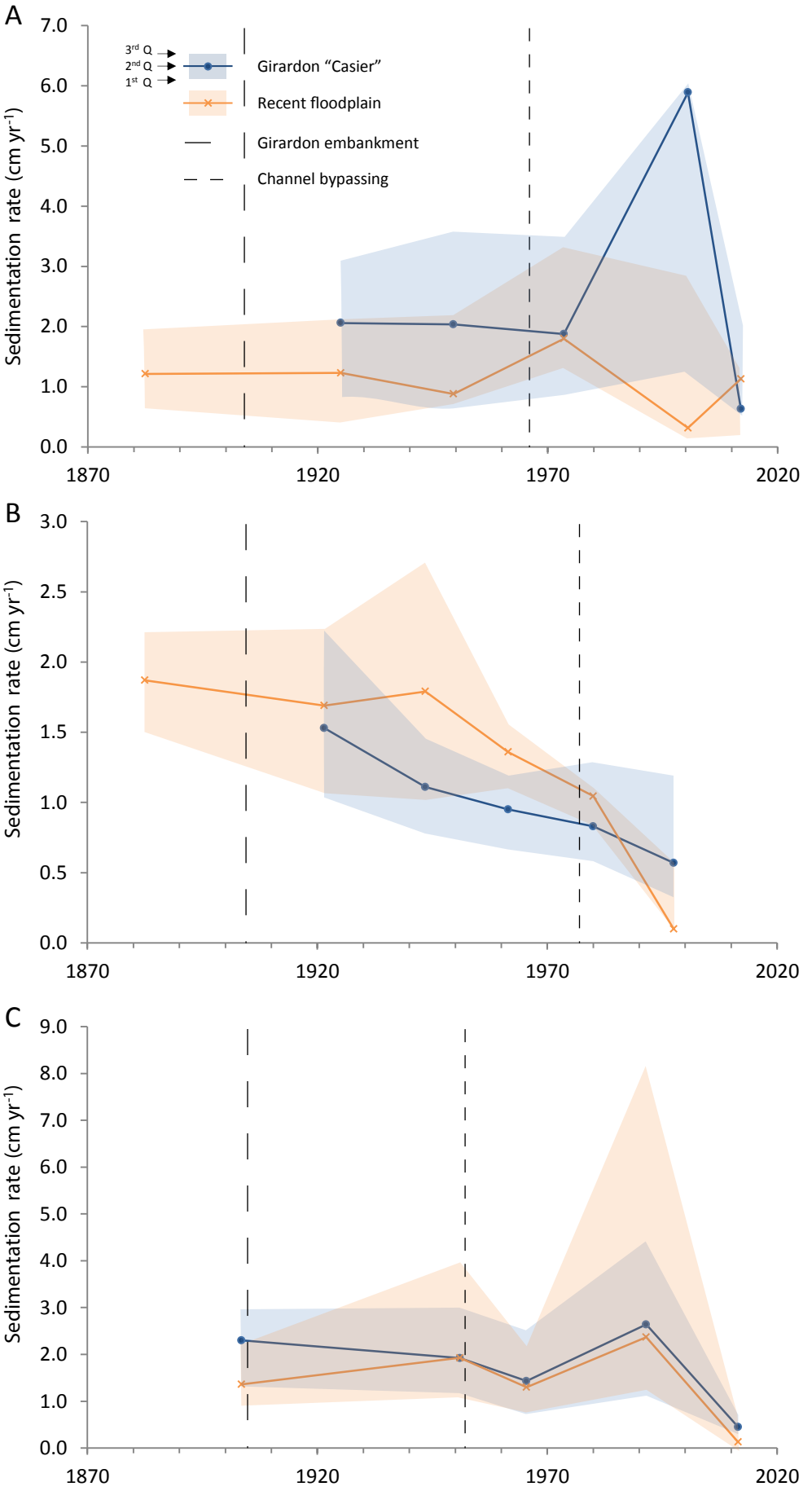
A
B
C
Sedimentation rate (cm yr-1)
3rd Q
2nd Q
1st Q
Girardon "Casier"
Recent floodplain
Girardon embankment
Channel bypassing
1870
1920
1970
2020

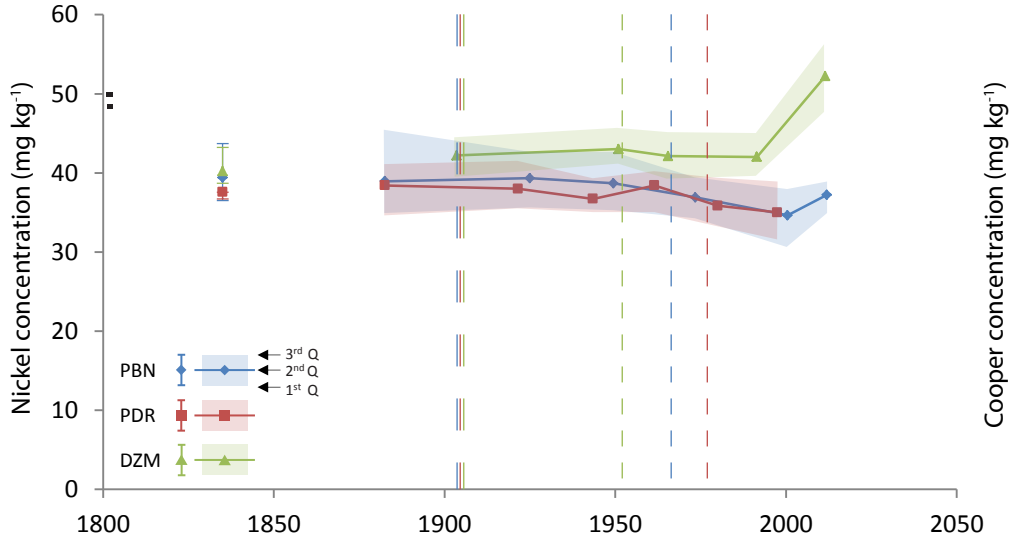
Nickel concentration (mg kg-1)
60
50
40
30
20
10
0
1800
1850
1900
1950
2000
2050
PBN
PDR
DZM
3rd Q
2nd Q
1st Q

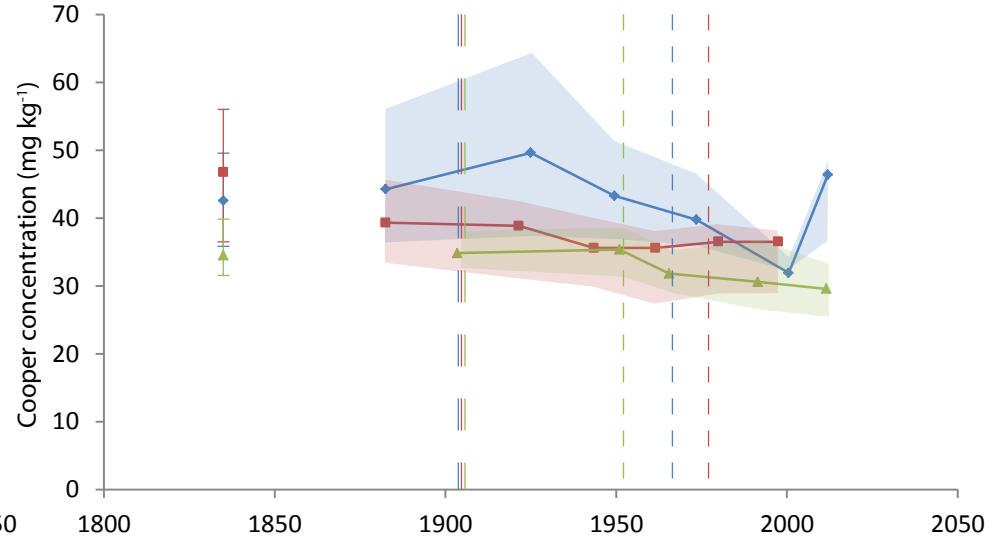
Cooper concentration (mg kg-1)
70
60
50
40
30
20
10
0
1800
1850
1900
1950
2000
2050

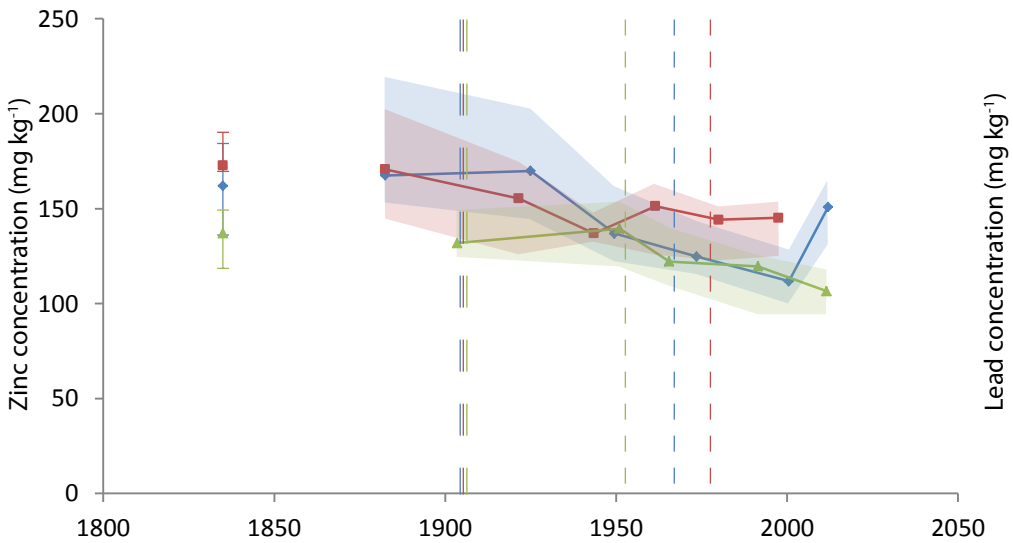
Zinc concentration (mg kg-1)
250
200
150
100
50
0
1800
1850
1900
1950
2000
2050

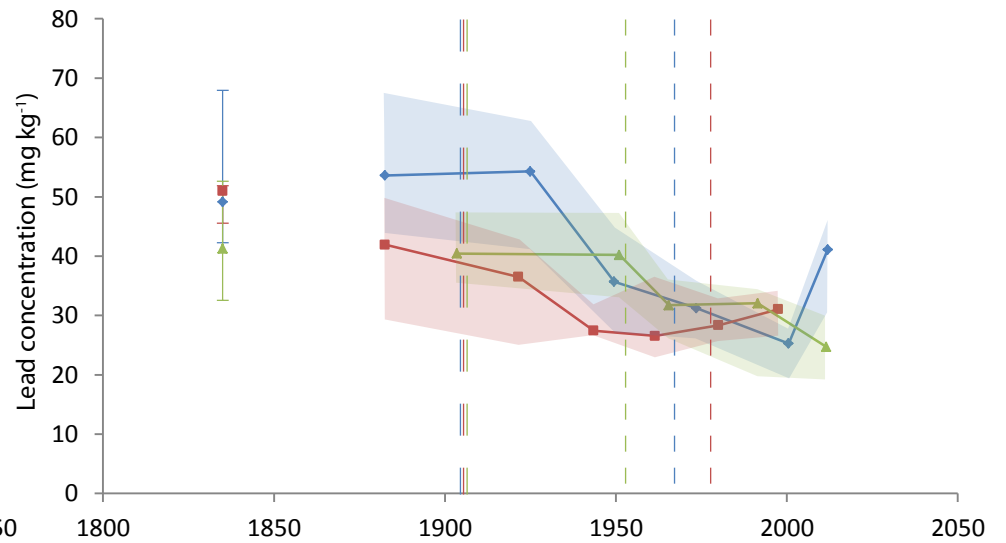
Lead concentration (mg kg-1)
80
70
60
50
40
30
20
10
0
1800
1850
1900
1950
2000
2050

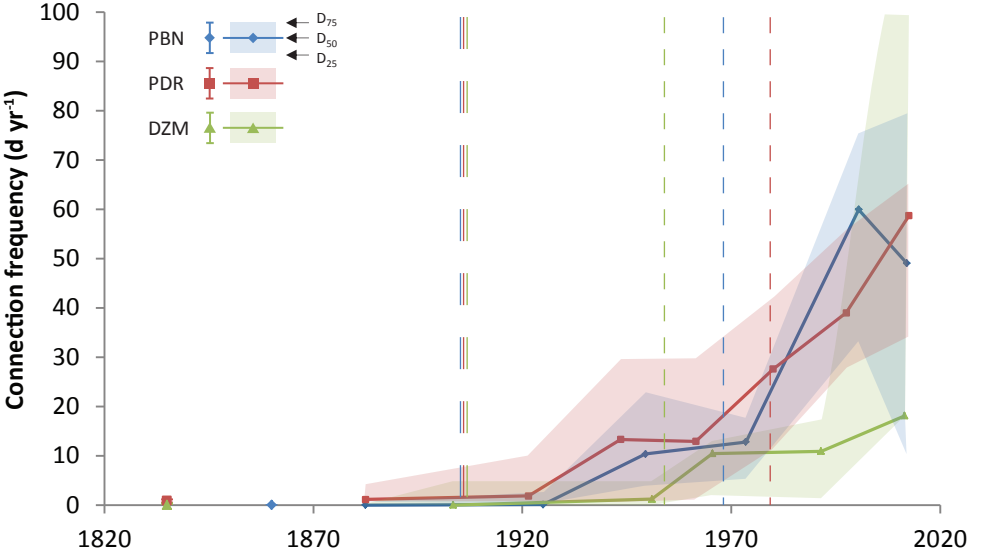
Connection frequency (d yr-1)
100
90
80
70
60
50
40
30
20
10
0
1820
1870
1920
1970
2020
PBN
PDR
DZM
D75
D50
D25

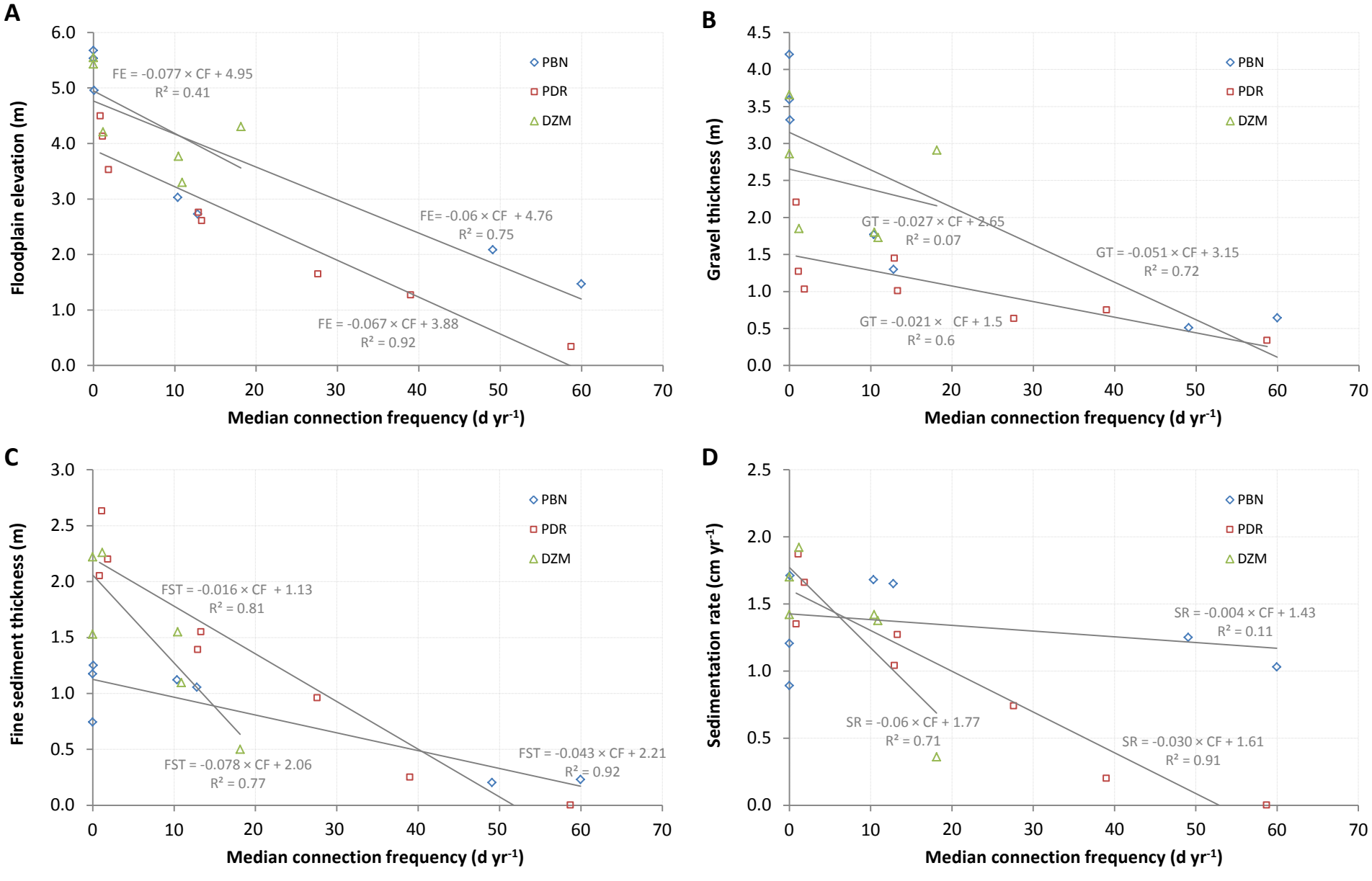
A
Floodplain elevation (m)
Median connection frequency (d yr-1)
PBN
PDR
DZM
FE = -0.077 × CF + 4.95
R² = 0.41
FE= -0.06 × CF + 4.76
R² = 0.75
FE = -0.067 × CF + 3.88
R² = 0.92
B
Gravel thickness (m)
Median connection frequency (d yr-1)
PBN
PDR
DZM
GT = -0.027 × CF + 2.65
R² = 0.07
GT = -0.051 × CF + 3.15
R² = 0.72
GT = -0.021 × CF + 1.5
R² = 0.6
C
Fine sediment thickness (m)
Median connection frequency (d yr-1)
PBN
PDR
DZM
FST = -0.016 × CF + 1.13
R² = 0.81
FST = -0.078 × CF + 2.06
R² = 0.77
FST = -0.043 × CF + 2.21
R² = 0.92
D
Sedimentation rate (cm yr-1)
Median connection frequency (d yr-1)
PBN
PDR
DZM
SR = -0.004 × CF + 1.43
R² = 0.11
SR = -0.06 × CF + 1.77
R² = 0.71
SR = -0.030 × CF + 1.61
R² = 0.91

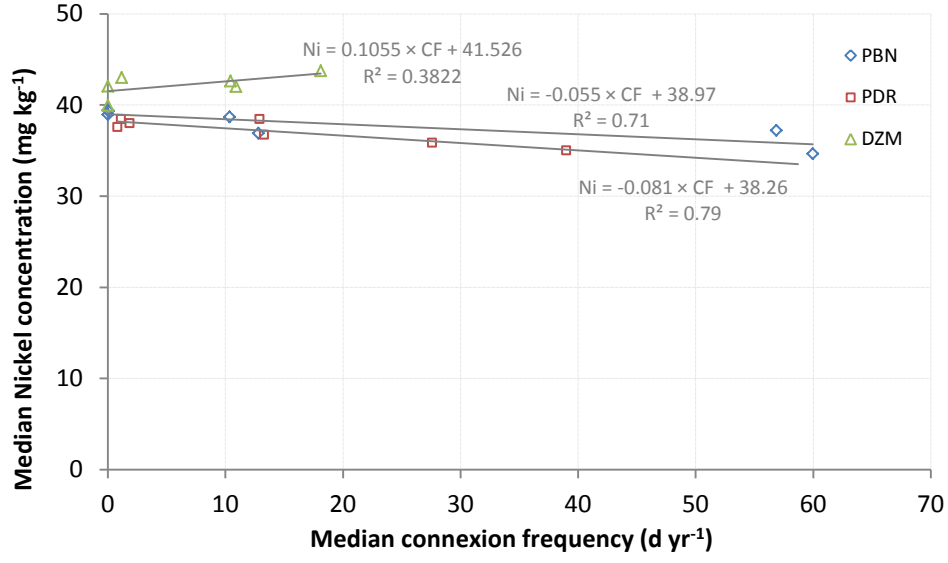
Median Nickel concentration (mg kg-1)
Median connexion frequency (d yr-1)
PBN
PDR
DZM
Ni = 0.1055 × CF + 41.526
R² = 0.3822
Ni = -0.055 × CF + 38.97
R² = 0.71
Ni = -0.081 × CF + 38.26
R² = 0.79

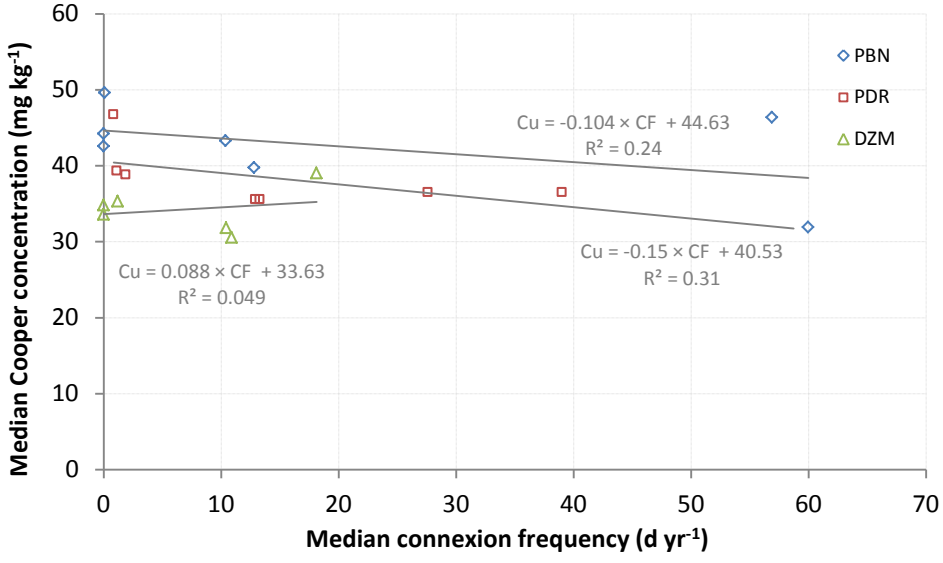
Median Cooper concentration (mg kg-1)
Median connexion frequency (d yr-1)
PBN
PDR
DZM
Cu = -0.104 × CF + 44.63
R² = 0.24
Cu = 0.088 × CF + 33.63
R² = 0.049
Cu = -0.15 × CF + 40.53
R² = 0.31

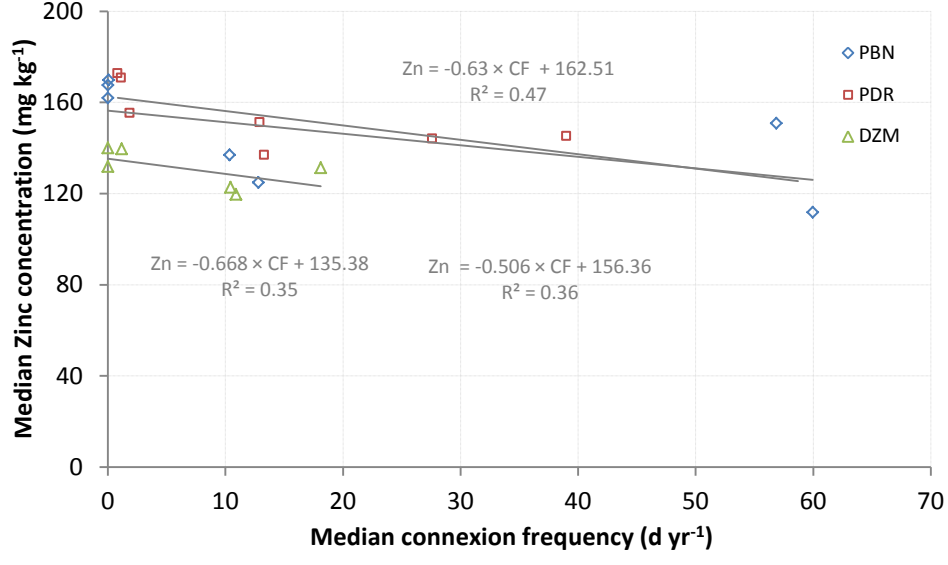
Median Zinc concentration (mg kg-1)
Median connexion frequency (d yr-1)
PBN
PDR
DZM
Zn = -0.63 × CF + 162.51
R² = 0.47
Zn = -0.668 × CF + 135.38
R² = 0.35
Zn = -0.506 × CF + 156.36
R² = 0.36

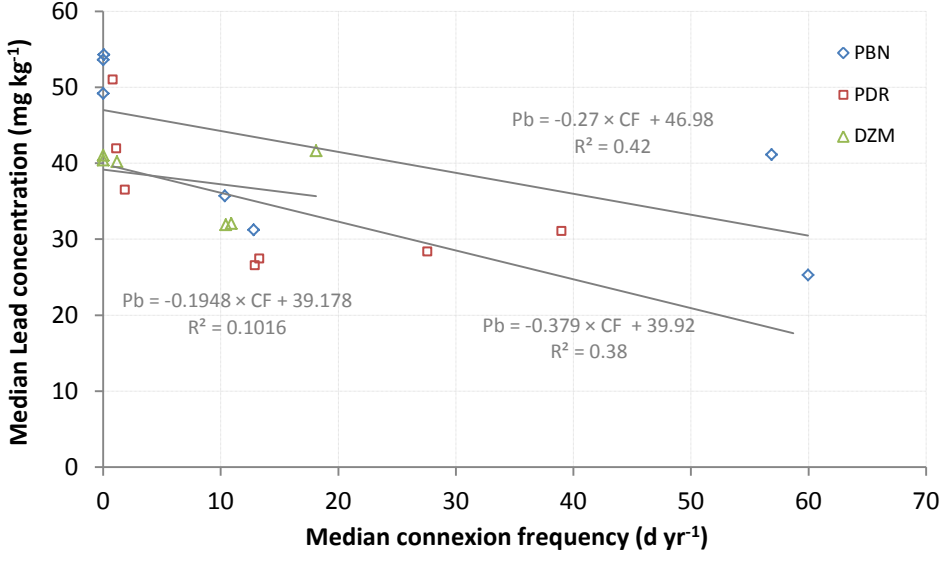
Median Lead concentration (mg kg-1)
Median connexion frequency (d yr-1)
PBN
PDR
DZM
Pb = -0.27 × CF + 46.98
R² = 0.42
Pb = -0.1948 × CF + 39.178
R² = 0.1016
Pb = -0.379 × CF + 39.92
R² = 0.38